Available online at www.sciencedirect.com
SCIENCE DIRECT
Dyes and Pigments 69 (2006) 151–176
DYES and PIGMENTS
www.elsevier.com/locate/dyepig

Photo-oxidation of pyrazolinylazo dyes and analysis of reactivity as azo and hydrazone tautomers using semiempirical molecular orbital PM5 method

Toshio Hihara [a,*], Yasuyo Okada [b], Zenzo Morita [c]

[a] Technical Center, DyStar Japan Ltd., Azuchi-machi 1-7-20, Chuo-ku, Osaka 541-0052, Japan
[b] School of Domestic Science, Otsuma Women's University, Sanban-cho, Chiyoda-ku, Tokyo 102-8357, Japan
[c] Tokyo University of Agriculture and Technology, Koganei, Tokyo 184-8588, Japan

Received 18 December 2004; accepted 18 February 2005
Available online 23 May 2005

Abstract

Photo-oxidative fading of seven pyrazolinylazo dyes was examined by exposing the dyed cellulose films immersed in an aerobic aqueous Rose Bengal solution to a carbon arc. The ease with which the dye was photo-oxidised was determined as k_0, the second-order rate constant of the reaction of the dye with singlet oxygen, from the initial rate of the fading. Calculating standard enthalpies of formation for the dyes in the gas phase and water by the PM5 method determined the azo–hydrazone tautomerism (AHT) of the dyes. Four dyes existed as a hydrazone tautomer (HT) and one dye as an azo tautomer (AT) in both phases without exhibiting AHT, and two dyes as HT in the gas phase and as an azo/keto tautomer (A/KT) in water. According to frontier orbital theory, the reaction sites for the corresponding tautomer(s) of azo dyes on cellulose to molecular singlet oxygen and their reactivity were analysed. The reaction sites were primarily the double bonds (C=N) of the hydrazone structure and other double bonds in the pyrazoline ring and secondarily several double bonds around carbon atoms connected with substituents. The probable reaction modes are ene and [2 + 2] cycloaddition toward the double bonds. These reaction modes were confirmed to be consistent with the absorption spectra of decomposed products combined with cellulose. The k_0-values obtained had a close correlation with the sum of Fukui's electrophilic frontier densities, $f_r^{(E)}$, at both atoms of the corresponding double bonds (i.e. a linear correlation between $\log k_0$ and the sum of $f_r^{(E)}$). The sum was demonstrated to be a molecular descriptor of the reactivity toward singlet oxygen of a molecule.

Keywords: Reactive dye; Reactivity toward singlet oxygen; Electrophilic frontier density; Ene reaction; [2 + 2] Cycloaddition; Molecular descriptor

1. Introduction

In a previous paper [1], the present authors analysed the azo–hydrazone tautomerism (AHT) of azobenzenes, phenylazopyrazolines and naphthalene diazo dyes in the gas phase and water using the semiempirical molecular orbital (MO) PM5 method. These procedures predicted that the AHT in both the gas and water phases occurs as follows: arylazobenzene dyes with *o*-amino, *o*-acetylamino or *o*-ureido groups exist as azo tautomers (ATs) in both the gas phase and water with some exceptions in the gas phase, while those with *o*-hydroxy groups exist as ATs in the gas phase and as hydrazone tautomers (HTs) in water. Due to the keto–enol tautomerism of the pyrazoline ring, three kinds of azo and hydrazone (azo/enol, azo/keto (A/K) and hydrazone/keto) tautomers

* Corresponding author. Tel.: +81 6 6263 6681; fax: +81 6 6263 6697.
E-mail address: hihara.toshio@dystar.com (T. Hihara).

0143-7208/$ - see front matter © 2005 Elsevier Ltd. All rights reserved.
doi:10.1016/j.dyepig.2005.02.018

exist in phenylazopyrazolinyl dyes. The AHT of azobenzenes and phenylazopyrazolines is simple and clear, while the AHT of other monoazo dyes derived from H-acid is considerably complex [2,3].

When this MO calculation procedure is applied to reactive dyes examined in the present study, all the reactive groups are assumed to react with hydroxyl groups, not with cellulose, although the dyes on cellulose must be bound with hydroxyl groups of cellulose. Neither effects of the glucose ring as the monomer unit nor the position of the hydroxyl group bound are taken into consideration. The authors make this assumption as a starting point to discuss the AHT and reactivity of reactive dyes in the cellulose–reactive dye system. The validity of this assumption is not further persuaded, although there may be problems that are debatable.

The absorption spectra of the reactive dyes bound with cellulose shifted to a longer wavelength compared with those in water. However, when dyed films were immersed in water, no effect of water was detected on the position of λ_{max}, although the intensity of absorption was changed due to expansion of the cellophane by swelling in area.

In order to settle this azo and/or hydrazone assignment problem, strict assignment of azo or hydrazone tautomer must be made in a phase where absorption spectra can be precisely measured, and quantum chemical assignment by MO calculation must be done with high accuracy. One may find no method with high reliability for the assignment, although very recent reports treated only the solvent effects on the λ_{max} of electronic spectra using semiempirical MO methods [4–7]. The authors considered that the pattern of absorption spectra even for fluorophors with simpler chemical structures was too complex to analyse theoretically in detail.

In other previous papers [3,8], on the other hand, the present authors discussed the reaction of azo and hydrazone tautomers (A&HTs) with singlet oxygen and revealed that A&HTs possess reactivities toward singlet oxygen that are similar to each other.

In the present paper, the photo-oxidation, or the reaction with singlet oxygen, of several yellow azo dyes is examined using dyed cellophane films, and their reaction sites and the corresponding reactivities of both the A&HTs are analysed using the semiempirical MO (PM5) method.

2. Experimental

2.1. Yellow dyes used

Seven pyrazolinylazo dyes were used in total, the A&HTs of almost all of which were analysed in a previous paper [1]. The chemical structures (except for Pyr-Yellow, the hydrazone tautomers are illustrated), C.I. generic name, C.I. constitution number, and abbreviations in parentheses are shown below:

(1) C.I. Reactive Yellow 2, hydrazone, C.I. 18972 (Yellow 2)

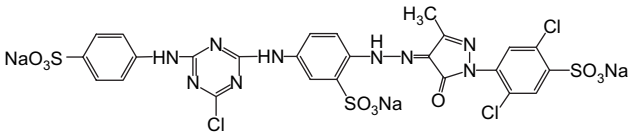

(2) C.I. Reactive Yellow 13, hydrazone, C.I. 18990 (Yellow 13)

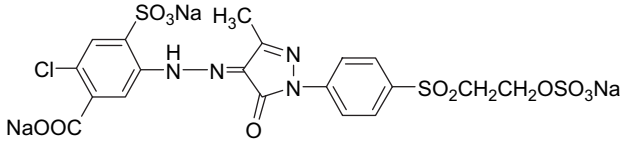

(3) C.I. Reactive Yellow 14, hydrazone, C.I. 19036 (Yellow 14)

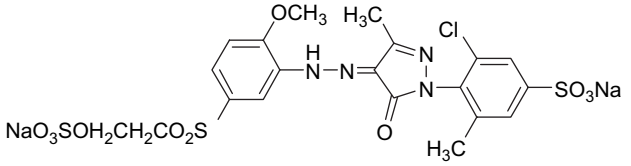

(4) C.I. Reactive Yellow 17, hydrazone, C.I. 18852 (Yellow 17)

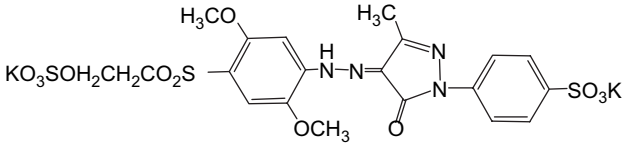

(5) An aminopyrazolinyl azo dye, azo (Pyr-Yellow)

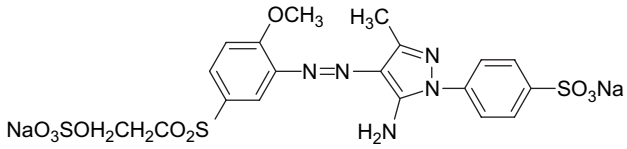

(6) A carboxypyrazolinyl azo dye, hydrazone (Carbopyr-Yellow)

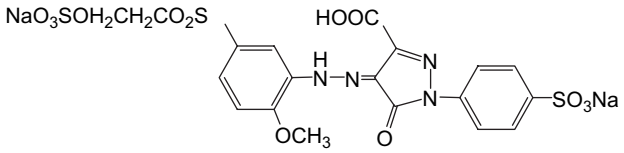

(7) A naphthylazopyrazolinyl dye, hydrazone (Naphpyr-Yellow)

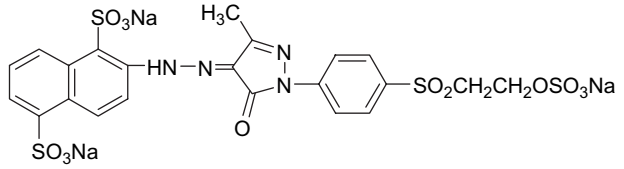

2.1.1. Numbering of atomic position

The numbers of atomic positions for individual dyes of the chemical structures described are shown below Tables 5 and 6, and are used in the text and other tables. They are different from the numbering used in IUPAC chemical nomenclature.

2.2. Dyeing of cellophane sheet

Cellophane films (Futamura Kagaku Kogyo K.K. #300), were scoured in boiling water for more than 2 h and dyed with each dye by the alkali-shock method to obtain an absorbance between 0.4 and 0.8 at the λ_{max} [9,10].

2.3. Estimation of ease with which dyes are photo-oxidised by the use of Rose Bengal

By exposing cellophane films dyed with reactive dyes to a carbon arc on immersing the dyed film in an aerated aqueous Rose Bengal solution, the relative fading of individual dyes was estimated [9,10]. Because reactive dyes combined with cellulose have different number of sulfonic acid groups and thus the adsorption of Rose Bengal on dyed cellulose is different from dyes especially in low concentrations of neutral salt, a high concentration of sodium sulfate (0.5 M) was added to the Rose Bengal solution. The solution was renewed every 5 h during exposure to keep the adsorption of Rose Bengal constant. From the initial rates of relative fading, A/A_0, where A_0 and A were the absorbance measured at the λ_{max} of each dye on the initial and exposed samples, respectively, the ease with which the dye was photo-oxidised was estimated as k_0 ($dm^3\,mol^{-1}\,s^{-1}$) values [9,10].

2.4. MO calculations

All MO calculations were made using CAChe MOPAC 2002 (Windows edition, Version 6.1.10) (Fujitsu Ltd.). For A&HTs as well as A/KTs of seven yellow dyes (and the model pyrazolinyl compounds in Schemes 1 and 2) in the gas phase and water, structure optimization was performed to obtain their molecular parameters such as standard heat of formation ($kcal\,mol^{-1}$), electron density at each atom in HOMO and LUMO, electrophilic frontier density, dipole moment and HOMO and LUMO energy using the PM5 method.

3. Results and discussion

3.1. Photo-oxidation of yellow reactive dyes or ease with which a dye is photo-oxidised by Rose Bengal

It is well known that one of the most common sources of singlet oxygen is energy transfer from an excited sensitizer such as Rose Bengal, Methylene Blue or phthalocyanines [11–15]. The sensitizer absorbs the light and is converted to an electronically excited singlet state and then to an excited triplet state. This state then transfers energy to oxygen, producing singlet oxygen and regenerating the sensitizer. Singlet oxygen can oxidise only dyes which exist nearby because the life of singlet oxygen is very short.

The photosensitised oxidative fading of each dye on cellulose film was drawn as relative fading profiles against the time of exposure, as illustrated in Fig. 1 (cf. Section 2.3). The fading of Pyr-Yellow was discussed in a previous study [16]. The order of the rate of fading was as follows:

$$\begin{aligned}&\text{Pyr-Yellow} \gg \text{Yellow 14} > \text{Yellow 2} \gg \text{Yellow 17}\\ &\quad \gg \text{Yellow 13} \gg \text{Carbopyr-Yellow}\\ &\quad > \text{Naphpyr-Yellow}\end{aligned} \tag{1}$$

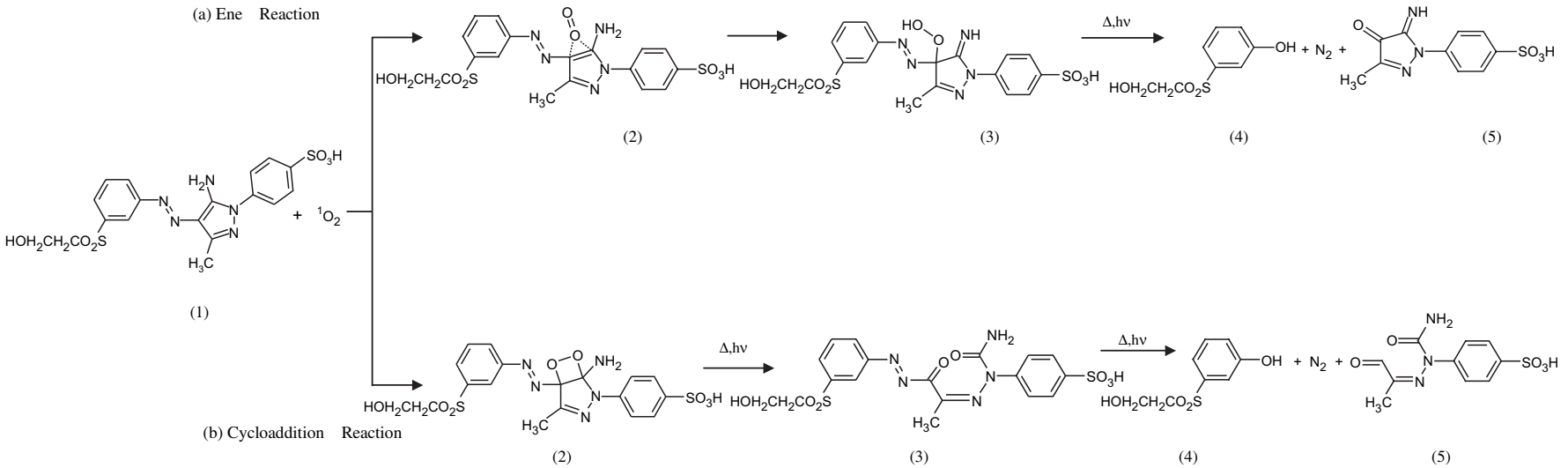

Scheme 1. (a) Ene (C1═C2; H(N20)) and (b) [2 + 2] cycloaddition (C1═C2) reactions of the ATs of a model aminopyrazolinylazo dye (**1**), which contains a vinylsulfonyl anchor in the diazo component, with singlet oxygen. In (a), (**2**): ene intermediate by the addition of singlet oxygen to the double bond at C1═C2, (**3**): the hydroperoxide via ene reaction, (**4**) and (**5**): thermal and/or photo decomposed products from the hydroperoxide via dediazotization, where some by-products other than (**4**) and (**5**) may be formed. In (b), (**2**): 1,2-dioxetane via [2 + 2] cycloaddition (the intermediate by the parallel addition of $^1O_2$ to the double bond of C1═C2 was omitted), (**3**) thermal and/or photo decomposed products from the 1,2-dioxetanes, scission of C1═C2 bond, (**4**) and (**5**): thermal and/or photo decomposed products from (**3**) via dediazotization, where some by-products other than (**4**) and (**5**) may be formed. The schemes for ATs can be also applied to those of A/KTs (see text).

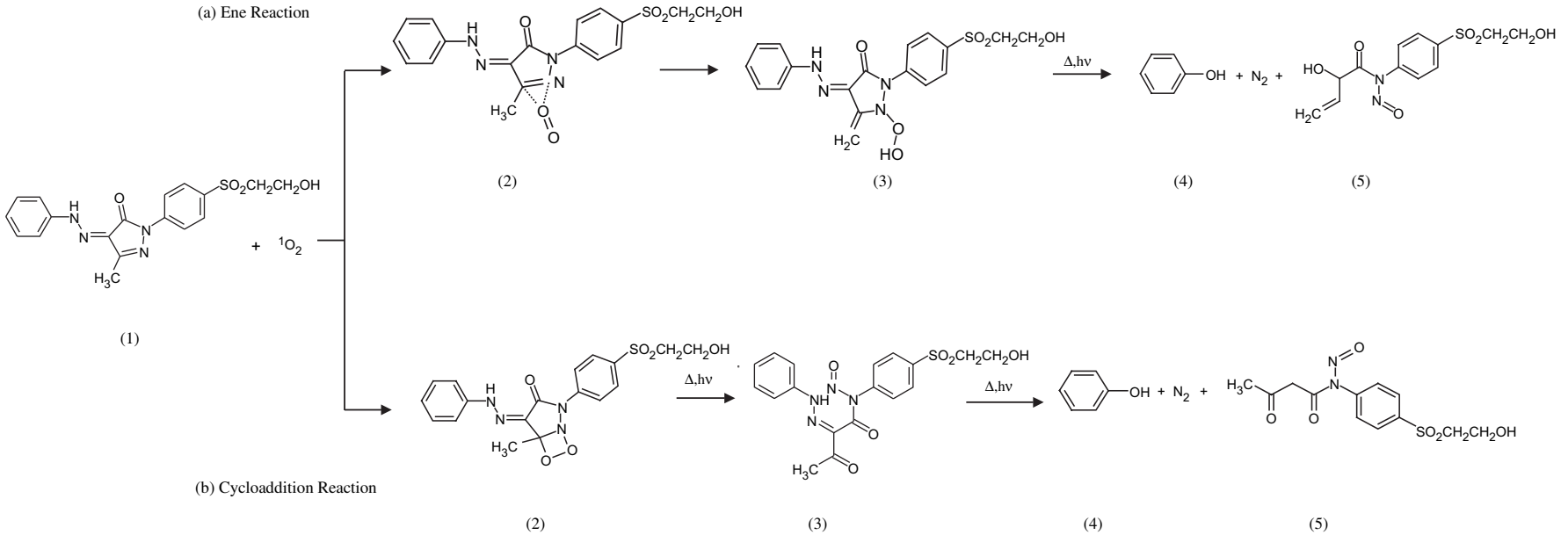

Scheme 2. (a) Ene (N4═C5; H(Me)) and (b) [2 + 2] cycloaddition (N4═C5) reactions of the ATs of a model aminopyrazolinyl azo dye (**1**), which contains a vinylsulfonyl anchor in the coupling component, with singlet oxygen. In (a), (**2**): ene intermediate by the addition of singlet oxygen to the double bond at N4═C5, (**3**): the hydroperoxide via ene reaction, (**4**) and (**5**): thermal and/or photo decomposed products from the hydroperoxide via dediazotization, where some by-products other than (**4**) and (**5**) may be formed. In (b), (**2**): 1,2-dioxetane via [2 + 2] cycloaddition (N4═C5) (the intermediate by the parallel addition of $^1O_2$ to the double bond of N4═C5 was omitted), (**3**) thermal and/or photo decomposed products from the 1,2-dioxetanes, scission of N4═C5 bond, (**4**) and (**5**): thermal and/or photo decomposed products from (**3**) via dediazotization, where some by-products other than (**4**) and (**5**) may be formed (see text).

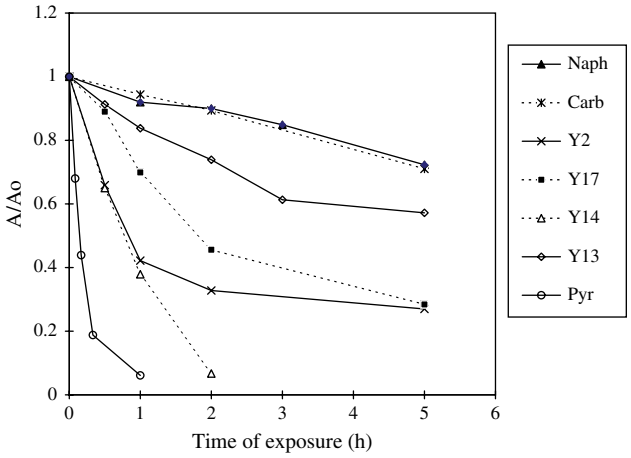

Fig. 1. Relative rates of photosensitive fading of pyrazolinylazo dyes on cellulose with Rose Bengal on exposure to carbon arc through Toshiba Y-51 filter.

Pyrazolinylazo dyes had a wide range of ease with which they were photo-oxidised, like the azo dyes examined previously [9,10].

The values of second-order rate constants, k_0 ($dm^3\,mol^{-1}\,s^{-1}$), for the reaction between dyes and singlet oxygen were estimated from the initial slope of fading illustrated in Fig. 1, using the previously determined k_0-value for Pyr-Yellow as the reference [16]. The results are listed in Table 1. Why pyrazolinylazo dyes possess such a wide range of reactivities is discussed next for each predominant tautomer.

3.2. Azo–hydrazone tautomerism on cellulose

The AHT of hydroxyazo and aminoazo dyes depends on the solvation or the environment in which the dyes exist. The standard enthalpies, $\Delta_f H^\circ$ ($kcal\,mol^{-1}$), of formation for these dyes in the gas phase and in water were estimated using the PM5 method as listed in Tables 2 and 3 and in previous papers [1–3]. The tautomers, which are supposed to exist predominantly from the values of $\Delta_f H^\circ$, are also summarised in Table 4. They coincided with the results of a previous study [1] except for Yellow 14 in water, although some dyes were newly added to the present study. Although the absolute values of $\Delta_f H^\circ$(gas) in the gas phase and $\Delta_f H^\circ(H_2O)$ in water for individual dyes were different depending upon the Hamiltonian (AM1, PM3 and PM5) and their versions of MOPAC, the MO calculations using these methods resulted in almost the same estimation of AHT.

Dyes having the same predominant tautomer in both phases according to the MO calculations can be regarded to exist as the same tautomer. When they showed different tautomers, however, one has unfortunately no procedure to describe the solvation effects of dyes in a solid polymer, but only in a pure liquid. In the present study, the photo-oxidative fading of dyes by Rose Bengal was examined under wet conditions or in water-swollen cellulose. The extent of solvation of dyes in polymers such as cellulose (dielectric constant $\varepsilon = 6.7$–7.5 (20–70 °C [17]) and nylon 6 ($\varepsilon = 3.3$–5.2 (30–60 °C [18])) may be in between the extent in the gas phase and in water, if the bulky hard segment of the polymer as well as dye–polymer interaction had no effect on the optimized structure of the dyes in the substrate. The absorption spectra of dyes on cellulose films, however, were not affected by the swelling with water except for the effects due to changes in the area of the films. Water, which acted as swelling agent, might have no effect on the solvation of dyes in the polymer. The extent of solvation in cellulose might be in between both the phases and the value of the dielectric constant closer to that of the gas phase because solvent effects appeared

Table 1
Values of the rate constant, k_0 ($dm^3\,mol^{-1}\,s^{-1}$), of the second-order reaction with $^1O_2$ estimated from the initial slope of relative fading, A/A_0, for yellow reactive dyes on cellulose immersed in aerated Rose Bengal (3.3×10^{-5} M + 0.5 M Na_2SO_4) solution on exposure to carbon arc through a Toshiba filter Y-51 (cf. Fig. 1), absorption spectra of decomposed products on cellulose, and light-related colour fastness of dyes

	Yellow dyes	k_0	Absorption spectra of the decomposed products on cellulose	Lightfastness on cotton[b] (1/6SD)	Perspiration-light fastness[c] (1/1SD)
1	Pyr-Yellow	6.9 [9]	Same as Yellow 14 and almost same as Carbopyr-Yellow	2	4.5
2	Yellow 13[a]	0.41	Similar to Naphpyr-Yellow	5	4.5
3	Yellow 14[a]	1.5_8	Same as Pyr-Yellow and almost same as Carbopyr-Yellow	3	4.5
4	Yellow 17[a]	0.76	Analogous to Pyr-Yellow and Yellow 14	4.5	4.5
5	Yellow 2[a]	1.4_6	Large two UV peaks (Triazine and 2 phenyls)	4.5	4.5
6	Carbopyr-Yellow	0.14_7	Almost same as Pyr-Yellow and Yellow 14	5	4.5
7	Naphpyr-Yellow	0.11_7	Similar to Yellow 13	5	4.5

[a] C.I. reactive generic name.
[b] Exposure to carbon arc.
[c] JIS L 0888, alkaline artificial perspiration, carbon arc.

Table 2
Enthalpy of formation $\Delta_f H^\circ$ (gas) (kcal mol^{-1}), dipole moment, μ (debye), HOMO and LUMO energies, E_{HOMO} and E_{LUMO} (eV), for azo, azo/keto, and hydrazone tautomers of yellow azo dyes in the gas phase, and $\Delta_f H^\circ(H_2O)$ for their tautomers in water, and electrophilic frontier density, $f_r^{(E)}$, for the most probable tautomer at the probable reaction sites, estimated by semiempirical molecular orbital PM5 method (cf. Tables 5 and 6)

Dye (Abbr.[a]) M.W.	Yellow 13 (Y13) 544.938			Yellow 14 (Y14) 544.981			Yellow 17 (Y17) 526.535			Pyr-Yellow (Pyr) 495.524		
	AT	A/KT	HT	AT	A/KT	HT	AT	A/KT	HT	AT	A/KT	HT
$\Delta_f H^\circ$(gas)	−237.123	−239.621	−240.054	−190.521	−192.878	−199.772	−215.733	−212.610	−223.610	−138.928	−126.950	−136.631
μ	4.889	9.233	7.531	6.554	6.532	8.443	5.876	7.865	4.367	7.423	11.346	4.289
E_{HOMO}	−9.591	−9.790	−9.745	−9.366	−9.290	−9.667	−9.515	−9.497	−9.550	−8.880	−9.214	−9.322
E_{LUMO}	−2.359	−2.350	−2.156	−1.643	−1.668	−1.654	−2.039	−1.925	−2.201	−1.557	−1.657	−1.406
$\Delta_f H^\circ(H_2O)$	−273.372	−280.719	−273.453	−216.882	−239.595	−247.941	−210.142	−219.984	−242.846	−182.557	−165.749	−173.953
$f_r^{(E)}$ (position for the most probable tautomer)	HT		A/KT	HT			HT			AT		
	0.082 (N4)		0.100 (C9)	0.137 (N4)			0.199 (C13)			0.457 (C1)		
	0.137 (C5)		0.134 (C8)	0.112 (C5)			0.058 (C8)			0.140 (C2)		
	0.176 (C15)		0.200 (C1)	0.106 (C1)			0.081 (N4)			0.093 (N6)		
	0.140 (C14)		0.050 (C5)	0.055 (N6)			0.077 (C5)			0.254 (N7)		
	0.183 (C19)		0.106 (N6)	0.100 (C15)			0.087 (C15)			0.164 (C8)		
			0.148 (N7)	0.048 (C14)			0.056 (C14)			0.085 (C13)		
	0.002 (C1)		0.071 (C12)	0.119 (C19)			0.088 (C19)			0.067 (C9)		
	0.026 (N6)		0.036 (C13)	0.052 (C8)			0.140 (C11)			0.056 (C10)		
				0.039 (C13)			0.033 (C12)					
			0.050 (C2)	0.111 (C16)			0.062 (C9)			0.160 (N4)		
			0.122 (N4)	0.039 (C17)			0.055 (C10)			0.021 (C5)		
				0.106 (C18)								
							0.058 (C1)					
							0.014 (N6)					

$f_r^{(E)}$ (position): electrophilic frontier density at the corresponding atomic position.
[a] Abbr. = Abbreviation used in Fig. 5.

Table 3
Enthalpy of formation, $\Delta_f H^\circ$(gas) (kcal mol^{-1}), dipole moment, μ (debye), HOMO and LUMO energies, E_{HOMO} and E_{LUMO} (eV), for azo, azo/keto, and hydrazone tautomers of yellow azo dyes in the gas phase, and $\Delta_f H^\circ(H_2O)$ for their tautomers in water, and electrophilic frontier density, $f_r^{(E)}$, for the most probable tautomer at the probable reaction sites, estimated by semiempirical molecular orbital PM5 method (cf. Tables 5 and 6)

Dye (Abbr.[a]) M.W.	Yellow 2 (Y2) 788.565			Carbopyr-Yellow (Carb) 526.492			Naphpyr-Yellow (Naph) 596.601		
	AT	A/K	HT	AT	K/T	HT	AT	A/KT	HT
$\Delta_f H^\circ$(gas)	−245.492	−248.415	−248.818	−254.771	−256.033	−261.698	−238.616	−241.475	−243.753
μ	4.566	4.863	9.881	9.086	8.322	8.643	4.395	5.160	4.832
E_{HOMO}	−9.564	−9.621	−9.702	−9.513	−9.552	−9.676	−9.636	−9.660	−9.849
E_{LUMO}	−2.303	−2.333	−2.113	−1.779	−2.298	−2.113	−2.248	−2.437	−2.391
$\Delta_f H^\circ(H_2O)$	−290.656	−293.256	−301.338	−309.283	−311.838	−318.198	−293.099	−302.768	−301.242
$f_r^{(E)}$ (position) for the most probable tautomer	HT		A/KT	HT			HT		A/KT
	0.071 (N4)		0.171 (C1)	0.091 (N4)			0.145 (C19)		0.225 (C1)
	0.071 (C5)		0.044 (C5)	0.112 (C5)			0.113 (C14)		0.048 (C5)
	0.086 (C11)		0.112 (C8)	0.112 (C15)			0.143 (C15)		0.079 (N6)
	0.045 (C12)		0.070 (C9)	0.075 (C14)			0.070 (N4)		0.159 (N7)
	0.019 (C13)		0.027 (C10)	0.115 (C19)			0.108 (C5)		0.093 (C11)
	0.055 (C8)		0.140 (C11)	0.046 (C13)					0.114 (C12)
	0.050 (C9)		0.081 (C12)	0.085 (C8)			0.046 (C8)		0.092 (C8)
	0.050 (C15)		0.044 (C13)				0.055 (C13)		0.114 (C13)
	0.050 (C14)		0.061 (N6)	0.169 (C1)			0.030 (C1)		
	0.136 (C19)		0.111 (N7)	0.031 (N6)			0.016 (N6)		0.146 (N4)
	0.056 (C16)			0.028 (C9)					0.014 (C2)
	0.067 (C17)		0.095 (N4)	0.072 (C10)					
	0.044 (C18)		0.010 (C14)						
	0.052 (C1)		0.006 (C2)						
	0.023 (N6)								
	0.106 (N7)								
	0.012 (C10)								

$f_r^{(E)}$ (position): Electrophilic frontier density at the corresponding atomic position.
[a] Abbr. = Abbreviation used in Fig. 5.

Table 4
Predominant tautomers in the gas and water phases estimated by $\Delta_f H°$(gas) and $\Delta_f H°(H_2O)$ using PM5 method, their probable primary mode of reaction for the tautomer with singlet oxygen (cf. Tables 2 and 3), and the atomic positions of their reactions

	Yellow dyes	Predominant tautomer (phase[c])	Probable primary mode of reaction (position)
1	Pyr-Yellow	AT(g and w)	AT: ene (C1=C2; H(N20), [2 + 2] cycloaddition (C1=C2, N6=N7, C8=C13, C9=C10), [[2 + 2] cycloaddition (N4=C5)][b]
2	Yellow 13[a]	A/KT(w) → HT(g)/A/KT(g)[d]	HT: ene (N4=C5; H(Me)), [2 + 2] cycloaddition (N4=C5, C14=C15, C14=C19), [ene (C1=N6; H(N7))][b] A/KT: [2 + 2] cycloaddition (C8=C9, C1=C5, N6=N7,C12=C13), [[2 + 2] cycloaddition (C1=C2, N4=C5)][b]
3	Yellow 14[a]	HT(g and w)	HT: ene (C1=N6; H(N7), N4=C5; H(Me)), [2 + 2] cycloaddition (N4=C5, C1=N6, C14=C15, C14=C19, C8=C13, C16=C17, C17=C18)
4	Yellow 17[a]	HT(g and w)	HT: [2 + 2] cycloaddition(C13=C8, N4=C5, C14=C15, C14=C19, C11=C12, C9=C10), ene (N4=C5; H(Me)), [ene and [2 + 2] cycloaddition (C1=N6)][b]
5	Yellow 2[a]	HT(w) → HT(g)/A/KT(g)[d]	HT: [2 + 2] cycloaddition (N4=C5, C11=C12, C12=C13, C8=C9, C14=C15, C14=C19, C16=C17, C17=C18, C1=N6), ene (C1=N6; H(N7)) [[2 + 2] cycloaddition (C10=C11)][b] A/KT: [2 + 2] cycloaddition (C1=C5, C8=C9, C10=C11, C12=C13, C8=C13, N6=N7), [[2 + 2] cycloaddition (C14=C19, C9=C10)][b]
6	Carbopyr-Yellow	HT(g and w)	HT: [2 + 2] cycloaddition (N4=C5, C14=C15, C14=C19, C8=C13), [ene (C1=N6; H(N7)), [2 + 2] cycloaddition (C1=N6, C9=C10)][b]
7	Naphpyr-Yellow	A/KT(w) → HT(g)	HT: [2 + 2] cycloaddition (N4=C5, C14=C15, C14=C19), [ene (C1=N6; H(N7)), [2 + 2] cycloaddition (C1=N6, C8=C13)][b] A/KT: [2 + 2] cycloaddition (C1=C5, C8=C13, C11=C12, N6=N7), [[2 + 2] cycloaddition (C9=C10)][b]

[a] C.I. reactive generic name.
[b] [ ]: Contribution of this reaction(s) is small to the k_0 values.
[c] g = Gas, w = H_2O.
[d] HT(g)/A/KT(g) = A mixture of HT(g) and A/KT(g) (HT dominant) in the gas phase.

dominantly in the region of a low dielectric constant [7]. It was regarded, therefore, in the present study that the extent of solvation in cellulose was approximated that in the gas phase (for the dyes whose predominant tautomers in both phases were different from each other, the reactivities of both tautomers are discussed).

3.3. Reactivity of yellow azo dyes in terms of frontier electron density estimated by MO method

Chemical reactions between singlet oxygen and various organic compounds have been revealed to have three different reaction modes providing (1) endoperoxides via [2 + 2] cycloaddition (Diels–Alder reaction), (2) dioxetanes or carbonyl fragments via [2 + 2] cycloaddition (dioxetane reaction) and (3) allylic hydroperoxides via 1,3-addition (ene reaction) [11,19–25]. In each reaction mode, several reaction mechanisms are known to be operative, although the preference of mechanisms is dependent on the experimental conditions. The mechanism may naturally depend upon the chemical structure of the dyes examined. Since systematic comparisons of their reactivity based on detailed analyses of the mechanism are impossible, a comparison of reactivity among the seven azo dyes examined is made in terms of frontier electron density based on the frontier orbital theory [26].

Fukui et al. [26–29] introduced a factor called the frontier electron density, f, which is the weighted sum of the squares of the coefficients of LCAO MO. The sum is weighted by the differences in energy from the frontier orbital (HOMO or LUMO). Fukui's original expression can be generalized for the three, electrophilic, nucleophilic and radical, reaction types as follows:

$$f_r^{(M)} = \frac{(2-\nu)\sum_{j=1}^{N} \nu_j \left(C_r^j\right)^2 \exp\left\{-\lambda\left(E_{\mathrm{HOMO}} - E_j\right)\right\}}{2\sum_{j=1}^{N} \nu_j \exp\left\{-\lambda\left(E_{\mathrm{HOMO}} - E_j\right)\right\}} + \frac{\nu\sum_{j=1}^{N} \left(2-\nu_j\right)\left(C_r^j\right)^2 \exp\left\{-\lambda\left(E_{\mathrm{LUMO}} - E_j\right)\right\}}{2\sum_{j=1}^{N} \left(2-\nu_j\right) \exp\left\{-\lambda\left(E_{\mathrm{LUMO}} - E_j\right)\right\}} \quad (2)$$

In this equation, (M) describes the reaction type: (E) for an electrophilic reaction, (R) for a radical reaction and (N) for a nucleophilic reaction; ν is a number indicating the type of reaction: 0 for an electrophilic reaction, 1 for a radical reaction and 2 for a nucleophilic reaction; N is the total number of orbitals; ν_j is the number of electrons

in the jth orbital and is usually 0, 1 or 2; C_r^j is the coefficient of the jth LCAO MO at the rth atomic position; E_j is the energy of the jth orbital; and λ is a scale factor that is usually set to 3.0 in these calculations [30]. Only the first term in the right-hand side of Eq. (2) contributes to $f_r^{(E)}$, the second term to $f_r^{(N)}$ and both the first and second terms to $f_r^{(R)}$. Fukui et al. [27] originally wrote Eq. (2) for the case of $N = 2$ and eliminated a factor of 2 in the denominator. In the simplest case, $f_r^{(M)}$ was described as follows [28]:

$$f_r^{(M)} = (2-\nu)\left(C_r^{\mathrm{HOMO}}\right)^2 + \nu\left(C_r^{\mathrm{LUMO}}\right)^2 \quad (3)$$

Thus, in the MOPAC program the quantity is divided by a factor of 2. In large molecules such as reactive dyes with some tens of orbitals, orbitals larger than $j = 2$ contribute to the quantity, although the contributions by the first (HOMO or LUMO) and/or the second highest or lowest orbitals are usually the largest.

In the photosensitised oxygenation reaction of azo dyes, HTs were separately reported to react with singlet oxygen via ene reaction [31,32]. According to the reports, several workers suggested that only the reaction of HTs with singlet oxygen is photofading [33–37]. Since azo dyes, which can exist only as ATs, also undergo photofading. ATs must suffer photosensitised oxidation, as was demonstrated using MO theory [3,8]. In the present study, the reactions of A&HT as well as A/KTs with singlet oxygen are discussed using the same procedure referring to the absorption spectra of decomposed products combined with cellulose (cf. Section 3.2).

3.4. Photodecomposed products of yellow azo dyes bound with cellulose

In a series of studies in which the photodecomposition of reactive dyes on cellulose was analysed, the authors [38–42] reported that the absorption spectra of decomposed products elucidated the existence of a residue of reactive anchors reacted with the cellulose substrate. The absorption spectra of samples exposed for seven dyes are discussed using the procedure of spectral analysis. The patterns of the absorption spectra of the decomposed products bound with cellulose were classified into several groups of reactive anchors as summarised in Table 1. (The reaction schemes with singlet oxygen are discussed in Section 3.6.)

Group A (Three pyrazolinylazo dyes with p-vinylsulfonylanisole anchor in diazo component): Yellow 14, Pyr-Yellow and Carbopyr-Yellow were synthesized by diazotizing 2-methoxy-5-(2-sulfatoethylsulfonyl)aniline and coupling with the corresponding pyrazolines. The decomposed products of the three dyes gave similar absorption spectra, although Carbopyr-Yellow showed some differences in the shape (Fig. 2). Coupling components had no effect on the spectra but did on the rates of the photo-oxidation reaction.

Group B (Two pyrazolinylazo dyes with N-(p-vinylsulfonylphenyl) anchor in coupling component): Yellow 13 and Naphpyr-Yellow belong to this group and seem to have similar shapes in the absorption spectra of decomposed products (Fig. 3).

Group C (Azo dye with 2,5-dimethoxy-4-(vinylsulfonyl)phenyl anchor in diazo component): Only Yellow 17 belongs to this group and has an additional 5-methoxy group compared to dyes of Group A (Fig. 4) (cf. Section 3.6.4).

Group D (Pyrazolinylazo dye from o-sulfo-p-phenylenediamine (diazo component) with 2-anilino-4-chlorotriazinyl anchor): Yellow 2 is composed of a phenyl ring bound with a large monochlorotriazinyl (MCT) anchor compared with the diazo component residue.

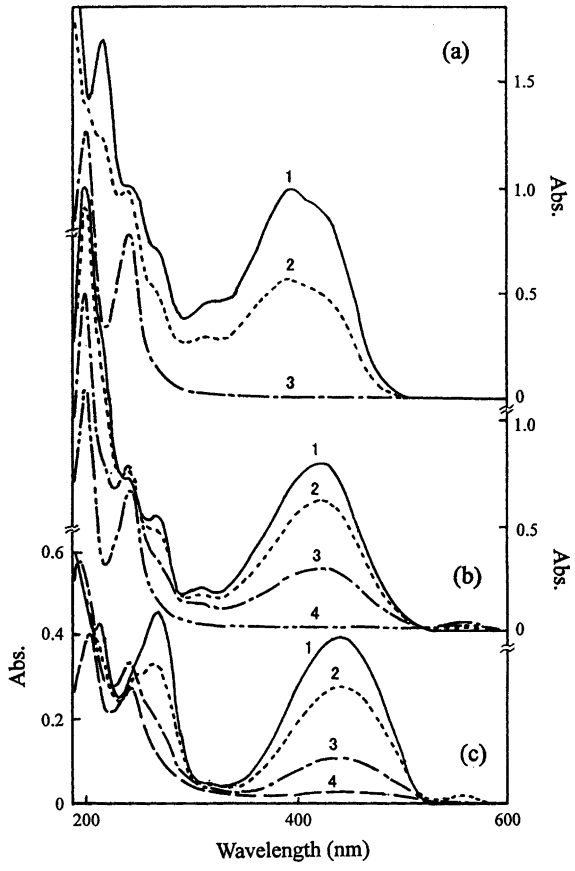

Fig. 2. Absorption spectra of the original dye (1) and of the decomposed products on cellophane film immersed in Rose Bengal solution after exposure to carbon arc through a Toshiba Y-51 filter for following times of exposure: (a) for Pyr-Yellow and exposure for 15 min (2) and 1 h (3) (completely decomposed product), (b) for Yellow 14 and the exposure for 0.5 h (2), 1 h (3) and 2 h (4) (completely decomposed product), (c) for Carbopyr-Yellow and exposure for 5 h (2) and 15 h (3) and the calculated spectrum (4) of the decomposed products reducing that of original one from the spectrum (3).

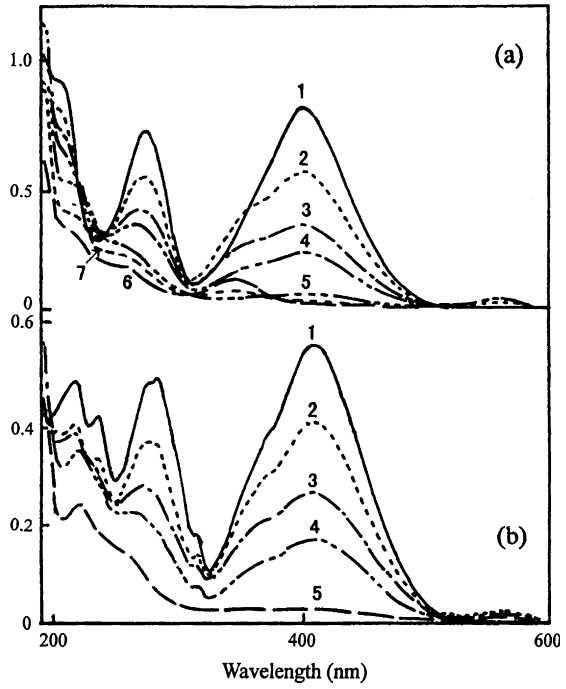

Fig. 3. Absorption spectra of the original dye (1) and of the decomposed products on cellophane film immersed in Rose Bengal solution after exposure to carbon arc through a Toshiba Y-51 filter for following times of exposure: (a) for Yellow 13 and exposure for 2 h (2), 5 h (3), 10 h (4) and 15 h (5), and the calculated spectra (6) and (7) of the decomposed products reducing that of the original one from the spectra (3) and (4), respectively, and (b) for Naphpyr-Yellow and their exposure for 5 h (2), 15 h (3) and 30 h (4), and the calculated spectrum (5) of the decomposed products reducing that of original one from the spectrum (4).

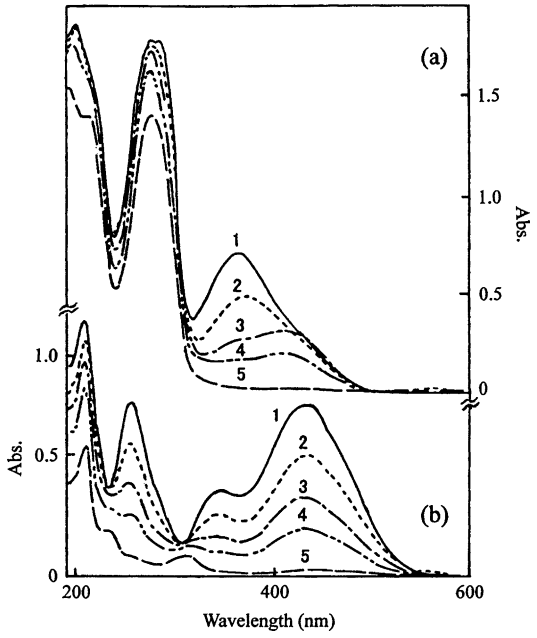

Fig. 4. Absorption spectra of the original dye (1) and of the decomposed products on cellophane film immersed in Rose Bengal solution after exposure to carbon arc through a Toshiba Y-51 filter for following times of exposure: (a) for Yellow 2 and exposure for 0.5 h (2), 1 h (3), 5 h (4) and 15 h (5) (completely decomposed product), and (b) for Yellow 17 and exposure for 1 h (2), 2 h (3), 5 h (4), and the calculated spectrum (5) of the decomposed products reducing that of original one from the spectrum (4).

3.5. Reaction scheme of azo dyes with singlet oxygen on the basis of frontier orbital theory

In the ene reaction of olefins having an allylic hydrogen with singlet oxygen the olefins are oxidised to allylic hydroperoxides concomitant with a shift of the double bond [11,19–25,43–53]. These allylic hydroperoxides are easily converted to allylic alcohols. Formation of a carbon–O_2 bond and removal of the hydrogen occurs on the same surface of the π-system and leads to exclusive formation of the trans olefinic linkage. Preferential hydrogen abstraction often occurs from sites germinal to the largest group, such as alkyl, sulfenyl, sulfinyl, sulfone and carbonyl groups. Thus, hydrogen abstraction from more than one site, a highly stereospecific superficial ene process, has been reported. Stephenson [43] suggested that an interaction between the LUMO of the oxygen and the HOMO of the olefin stabilises the transition state of the perepoxide-like intermediate. This intermediate formation, a stepwise mechanism, was demonstrated to occur in the rate-determining step [44,45], while a concerted mechanism was excluded [46,47]. The photo-oxidation of azo dyes with singlet oxygen was supposed to occur at the atomic position with the largest electron density of HOMO [3,8,21,48].

Besides the ene reaction, because two double bonds are fixed in a pyrazoline ring, singlet oxygen performs a [2 + 2] cycloaddition reaction with the constituent atoms of the double bond to give 1,2-dioxetanes, which are thermally decomposed into two carbonyl fragments or ring opening accompanying the formation of two carbonyl groups [51–65]. Some studies on the reactions of pyrazolines with singlet oxygen were reported [66–68]. It seems to have not yet been clarified whether ene or [2 + 2] cycloaddition reaction occurs on pyrazolinyl double bonds to which amino or methyl groups are attached or on olefins with allylic hydrogen or not.

According to frontier orbital theory, the reaction with singlet oxygen occurs at the position of the atom with the largest electron density, d_{HOMO}, of HOMO, and the reactivity may be proportional to the $f_r^{(E)}$ values, although what reaction mode at the position of the second largest $f_r^{(E)}$ values is used should be determined by the experimental results. Moreover, singlet oxygen may act as a biradical against such double bonds unlike the usual ionic reagents, and attack two neighbouring atoms with higher $f_r^{(E)}$ values. The electrophilic reactivity

of the double bonds toward singlet oxygen may be described by the sum, $S^{(E)}_{m,n}$, of the reactivities of the two atomic positions as follows:

$$S^{(E)}_{m,n} = \sum_{m,n} \left\{ f^{(E)}_m + f^{(E)}_n \right\} \quad (4)$$

where m and n denote the atomic positions of the corresponding double bonds, and when overlapped, the overlapped position is counted only once. Double bonds with a larger value of $(f^{(E)}_m + f^{(E)}_n)$ are taken into consideration one by one. Singlet oxygen, however, has no reactivity toward isolated atomic positions with higher $f^{(E)}_r$ values, such as nitrogen imino bridge groups and oxygen of sulfonate groups. The summation of Eq. (4) should be performed from the position with the largest value of $(f^{(E)}_m + f^{(E)}_n)$ to the site of the reaction limit. The $S^{(E)}_{m,n}$ values may describe the reactivity of a dye against singlet oxygen, a molecular descriptor for ene and/or [2 + 2] cycloaddition reactions.

In order to confirm whether or not these MO theories apply to the ene and/or [2 + 2] cycloaddition reactions of the A&HTs with singlet oxygen, the $S^{(E)}_{m,n}$ values given by Eq. (4) as the sum of $f^{(E)}_r$ value for the two atoms forming the double bond, which singlet oxygen may attack, were plotted against the $\log k_0$ values determined, as shown in Fig. 5. Formally, this relationship between $S^{(E)}_{m,n}$ values and $\log k_0$ has the same functional relation as the Hammett equation [69] and may be an extension of the multi-substituent effects, although there is no reference compound.

The possibilities of the reaction modes and their primary positions are summarised in Table 4. Taking all the possibilities into consideration, the positions of the ordinate were determined or fixed by experiments, while those of the abscissa were determined so as to find the general correlation between the $\log k_0$ values and the $S^{(E)}_{m,n}$ values. The course of analyses for individual dyes is explained next.

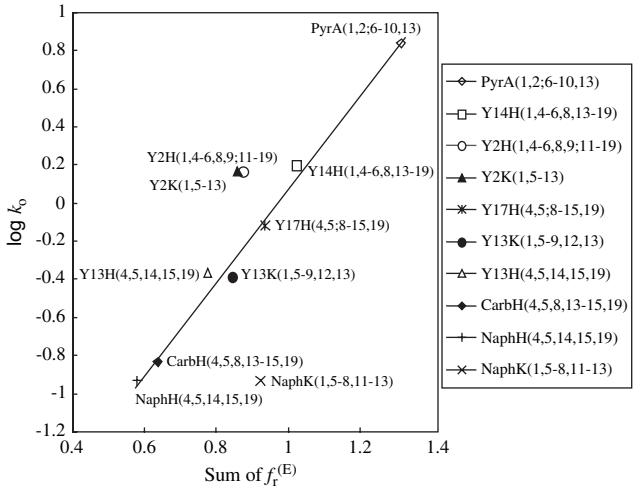

Fig. 5. Relationship between $\log k_0$ and $S^{(E)}_{m,n}$-values (the sum of $f^{(E)}_r$, Eq. (4)) for a series of pyrazolinylazo dyes (see text). (Symbols for dyes: Tables 2 and 3, symbols for tautomers: A: AT, H: HT, and K: A/KT).

3.6. Reaction modes of pyrazolinylazo dyes with singlet oxygen and thermal and/or photo decomposition of intermediates

The reactions of pyrazolinylazo dyes with singlet oxygen may generate decomposed products of definite structures, implying that these reaction mechanisms involved are ionic and not radical. The reactions are pericyclic ones and very selective. However, singlet oxygen is not only highly reactive but also of a biradical character. The reaction mechanisms and their modes toward azo dyes as well as their reaction sites, therefore, usually become more than single-track. The main reactions in the individual formation and decomposition reactions may occur preferentially. Since the reaction products formed by these primary reactions may suffer further photo and/or thermal decomposition reactions, which usually also become more than single-track, the decomposed products bound to cellulose through reactive anchor groups are a mixture of more than one end product. The validity of the reaction mechanisms may be analysed by the main component of the decomposed products. Because more than two components may be also contained in the end products on cellulose, the reaction mechanisms are discussed over more than single-tracks. In the case of azo dyes, since the primary reaction site is the coupling position, which may be one of the weakest points for colourfastness against chemical attacks, the clearer the reaction mechanism becomes, the larger the short-comings, and vice versa.

The thermal or photo elimination of N_2 from azo compounds, which occurs during the decomposition of the reaction intermediates, was reviewed as dediazotization [70–75]. It is utilized in imaging technology [72–74] and as an initiator of radical reaction [76]. It has also been treated theoretically using the MO method [77]. Depending on the experimental conditions, diazo compounds undergo several reactions such as hydro- (replacement of a diazo group by hydrogen), hydroxy- (formation of phenol), halogeno- and cyano-dediazotization [72,75]. And in dye chemistry, the ene reaction of HTs with singlet oxygen was studied [31–37] and enlarged to include all the tautomers of azo dyes [3,8] as well as [2 + 2] cycloaddition of azo dyes in the present study.

Since exposure continues to perform photosensitised oxygenation in this study, thermal and photo decompositions may occur concurrently with the formation of dioxetanes. As mentioned below, Yellow 13,

Carbopyr-Yellow and Naphpyr-Yellow yielded a small amount of reaction intermediates to end products during exposure. Thus, a few intermediates were supposed to occur in practice, although they are not illustrated in the schemes.

The pyrazolinylazo dyes examined possess many double bonds that can react with singlet oxygen via ene and/or [2 + 2] cycloaddition, and moreover, these reactions at various sites and their decomposition reactions giving more than one product may occur simultaneously. As representatives, the schemes of ene and [2 + 2] cycloaddition reactions at the double bonds of C1=C2 for the ATs of respective model compounds are illustrated in Scheme 1(a) and (b), while the schemes of the corresponding reactions at those of N4=C5 for the HTs are shown in Scheme 2(a) and (b). The ene reaction starting with an azo dye (**1**) toward singlet oxygen, drawn in Schemes 1(a) and 2(a), may generate a hydroperoxide (**2**), a labile intermediate, followed by further photolysis and/or thermolysis, resulting in the corresponding phenol (**3**), one of the end products, and oxidised aromatics (**4**) via dediazotization, according to the previous Refs. [8,30,31,48]. On the other hand, the [2 + 2] cycloaddition reaction, drawn in Schemes 1(b) and 2(b), may generate 1,2-dioxetane (**2**) [51–65], resulting in the ring opening of the dioxetane to form carbonyl fragments (**3**) by photolysis and/or thermolysis and followed by further photolysis and/or thermolysis to give the corresponding phenol (**4**), one of the end products, and oxidised aromatics (**5**) via dediazotization. (Compound (**5**) has a possibility of forming 4-vinylsulfonyl-2-nitroso-1-(substituted amino)benzene via Fischer–Hepp rearrangement, certainly if treated in HCl [78]. However, since this was not the case, the formation was not pursued.) When the diazo component contained a reactive anchor group, the decomposed products, one of which was a phenol, bound with cellulose through the anchor system may be observed in the absorption spectra (Scheme 1 as an example). When the coupling component possessed the anchor group, oxidised fragments of dye chromophore bound with cellulose through the anchor system may be observed in the absorption spectra (Scheme 2 as an example). Ene and [2 + 2] cycloaddition may give the same end product bound with cellulose. In practice, since the dyes examined possess more than one reactive double bond, the end products may be a mixture from these concurrent reactions. In conclusion, the [2 + 2] cycloaddition (C*m*=C*n*) (*m*,*n*: same meaning as in Eq. (4)) of either one of which connects to a bridge group such as azo and imino may generate 1,2-dioxetanes that result in the corresponding ring-opened decomposed products via dediazotization followed by the scission of the C–N bond, and in the case of ene reaction, similar bond scission may occur.

3.6.1. Reaction of ATs for Pyr-Yellow

Since a model aminopyrazolinyl azo dye, whose chemical structure is illustrated as (**1**) in Scheme 1, exists predominantly as ATs in the gas phase ($\Delta_f H^\circ$(gas) = −103.141 kcal mol^{-1} for the ATs and −98.538 kcal mol^{-1} for the HTs, respectively), the reaction scheme of only the ATs for this compound is illustrated to explain the scheme of the ATs of the series of pyrazolinylazo dyes examined. The $\Delta_f H^\circ$(gas) values of the end product as well as the values of corresponding transition state intermediate are shown in Tables 7 and 8.

There is much debate about the AHT of this dye in the gas phase as well as on cellulose left to discuss, although no one has a procedure to settle it. At present, the absorption spectra of reactive dyes with solubilising groups cannot be measured in the gas phase. No procedure has been found to calculate the electronic spectrum in a solid polymer with a low dielectric constant using the MO method.

As mentioned above, because singlet oxygen may conduct ene and [2 + 2] cycloaddition reactions with pyrazolinylazo dyes, which reactions occur predominantly and which ones are excluded should be analysed. In order to clarify these situations, ene and [2 + 2] cycloaddition reactions at the double bonds of C1=C2 (for ATs), C1=N6 (for HTs), N4=C5 (for A&HTs), C1=C5 (for A/KTs), etc. were analysed by calculating the enthalpy of formation for the predominant tautomers of the azo dyes examined: the reactants, intermediates and products, as well as the intermediates at the transition state geometry (TSG), using the PM5 method. Besides the double bonds in coupling component, Table 6 shows that double bonds: C8=C13 and C9=C10 possess considerable values of d_{HOMO} indicating potential reactivity toward singlet oxygen. The [2 + 2] cycloaddition at these two double bonds was also discussed. The values of $\Delta_f H^\circ$(gas) at the TSG may correspond to the saddle point between the reactant (starting material) and the corresponding intermediate in the reaction coordinate.

Scheme 1(a) and (b) describes the ene reaction and [2 + 2] cycloaddition, respectively, at the double bond of C1=C2 for the ATs of a model compound with singlet oxygen, which are applicable only to the ATs of Pyr-Yellow. The probable reaction modes for the predominant tautomers are summarised in Table 4 as ene (ATs; C1=C2; H(N20)), which describes the ene reaction performing the addition of singlet oxygen to the double bond between C1 and C2 and the abstraction of hydrogen from the amino group of N20 (see Section 2.1.1 for the numbering of atomic sites). The electron density of HOMO had the largest value at the C1 atom, the same situation as ATs of almost all dyes examined (cf. Tables 2, 3, 5 and 6). The $f_r^{(E)}$ values, which describe the electrophilic

Table 5
Electron density, d_{HOMO}, of HOMO at each atomic position for azo, azo/keto and hydrazone tautomers of Yellow 13, Yellow 14, Yellow 17 and Yellow 2 in the gas phase, calculated using PM5 method

	Yellow 13			Yellow 14			Yellow 17			Yellow 2		
	AT	AK	HT	AT	AK	HT	AT	AK	HT	AT	AK	HT
C1	0.223	0.149	0.007	0.130	0.166	0.070	0.062	0.010	0.083	0.174	0.137	0.030
C2	0.033	0.010	0.028	0.038	0.007	0.028	0.019	0.002	0.018	0.013	0.005	0.023
N3	0.047	0.032	0.265	0.025	0.024	0.219	0.137	0.002	0.102	0.033	0.020	0.160
N4	0.036	0.087	0.047	0.025	0.097	0.123	0.071	0.002	0.066	0.034	0.074	0.067
C5	0.019	0.034	0.088	0.010	0.063	0.105	0.052	0.004	0.041	0.039	0.033	0.065
N6	0.027	0.036	0.010	0.121	0.056	0.037	0.009	0.034	0.010	0.026	0.025	0.016
N7	0.143	0.080	0.008	0.180	0.081	0.109	0.112	0.045	0.150	0.100	0.071	0.064
C8	0.069	0.101	0.000	0.147	0.148	0.008	0.029	0.053	0.036	0.087	0.092	0.020
C9	0.080	0.078	0.000	0.043	0.033	0.001	0.000	0.049	0.007	0.080	0.057	0.022
C10	0.007	0.016	0.000	0.058	0.058	0.001	0.024	0.112	0.019	0.015	0.015	0.010
C11	0.105	0.117	0.000	0.054	0.047	0.000	0.068	0.128	0.089	0.128	0.124	0.035
C12	0.044	0.054	0.000	0.001	0.001	0.001	0.007	0.054	0.006	0.054	0.066	0.016
C13	0.036	0.026	0.000	0.063	0.059	0.010	0.100	0.264	0.112	0.029	0.036	0.009
C14	0.007	0.004	0.089	0.000	0.000	0.019	0.023	0.000	0.018	0.002	0.000	0.041
C15	0.008	0.004	0.083	0.000	0.000	0.012	0.033	0.000	0.026	0.000	0.001	0.006
C16	0.000	0.000	0.005	0.000	0.000	0.011	0.000	0.000	0.000	0.000	0.000	0.021
C17	0.012	0.006	0.149	0.000	0.000	0.019	0.048	0.001	0.038	0.004	0.002	0.058
C18	0.000	0.000	0.005	0.000	0.000	0.004	0.000	0.000	0.000	0.000	0.000	0.010
C19	0.009	0.004	0.087	0.001	0.001	0.032	0.035	0.000	0.027	0.005	0.001	0.100
O20	0.021	0.054	0.085	0.025	0.054	0.054	0.086	0.004	0.025			
N35										0.081	0.104	0.028

The numbers of atoms in the chemical structures are shown below. Yellow 13: $R_1 = SO_3H$; $R_2 = Cl$; $R_3 = COOH$; $R_4 = R_5 = R_7 = H$; $R_6 = SO_2CH_2CH_2OH$. Yellow 14: $R_1 = OCH_3$; $R_2 = R_5 = H$; $R_3 = SO_2CH_2CH_2OH$; $R_4 = CH_3$; $R_6 = SO_3H$; $R_7 = Cl$. Yellow 17: $R_1 = R_3 = OCH_3$; $R_2 = SO_2CH_2CH_2OH$; $R_4 = R_5 = R_7 = H$; $R_6 = SO_3H$. Yellow 2: $R_1 = R_6 = SO_3H$; $R_2 = 4$-(*p*-sulfoanilino)-6-hydroxytriazin-2-ylamino(N35); $R_3 = R_4 = H$; $R_5 = R_7 = Cl$.

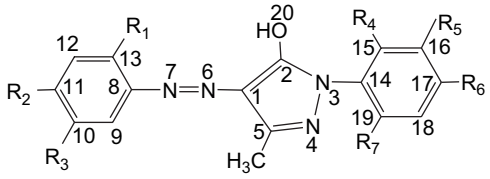

reactivity given by Eq. (2), for the primary mode of reaction: ene (ATs; C1=C2; H(N20)) are listed in Table 2 as 0.457 (C1) and 0.140 (C2), the sum of which, $S^{(E)}_{m,n}$ (*m*,*n*: 1,2), was largest among the ene reactions against all the individual double bonds of dyes used, as shown in Tables 2 and 3. The largest value corresponds also to the largest k_0 value of this dye. The $f_r^{(E)}$ values for the ene (N4=C5; H(Me)) in Table 2, were 0.160 (N4) and 0.021 (C5), while the values of d_{HOMO} in Table 6 were 0.085 (N4) and 0.002 (C5), respectively. Thus, the contribution of this mode to the k_0 value of Pyr-Yellow may be regarded as too small to estimate due to the very small value of $f_r^{(E)}$ at C5 in spite of the large one at N4. (Taking the lower limits of $f_r^{(E)}$ and d_{HOMO} into consideration, the double bonds which may react with singlet oxygen are mentioned below.)

The double bonds, C1=C2 and N4=C5, possess also the possibility of performing [2 + 2] cycloaddition, besides ene reaction. In order to speculate whether either one or both of ene and [2 + 2] cycloaddition reactions occur, the values of $\Delta_f H^\circ$(gas) for the corresponding reaction intermediates at TSG were calculated by the PM5 method. As mentioned above, the double bonds, C8=C13 and C9=C10, may perform [2 + 2] cycloaddition. The values of $S^{(E)}_{m,n}$ (*m*,*n*: 8,13) and $S^{(E)}_{m,n}$ (*m*,*n*: 9,10) come next to $S^{(E)}_{m,n}$ (*m*,*n*: 1,2) and are followed by the reactivity at N4=C5 which may be actually negligible. The results of enthalpy analyses for the ene and [2 + 2] cycloaddition reactions at probable positions are listed in Tables 7–9. The values of activation energies for the ene and [2 + 2] cycloaddition reactions for the predominant tautomers of all dyes examined were nearly equal to each other but a small difference between reaction modes irrespective of the A&HTs (Table 7) was observed. Moreover, the $\Delta_f H^\circ$(gas) of the intermediates at TSG had no reasonable relation with the $\Delta_f H^\circ$(gas) of hydroperoxides for ene reaction and that for [2 + 2] cycloaddition products. Thus, for all the dyes examined, no one can decide whether ene or [2 + 2] cycloaddition reactions occur dominantly, because the values of $S^{(E)}_{m,n}$ identify no dominance between them. Tables 7 and 8 also indicate small differences in the activation energies for

Table 6
Electron density, d_{HOMO}, of HOMO at each atomic position for azo, azo/keto and hydrazone tautomers of Pyr-Yellow, Carbopyr-Yellow and Naphpyr-Yellow in the gas phase, calculated using PM5 method

	Pyr-Yellow			Carbopyr-Yellow			Naphpyr-Yellow		
	AT	AK	HT	AT	AK	HT	AT	AK	HT
C1	0.269	0.200	0.120	0.131	0.085	0.093	0.207	0.168	0.006
C2	0.078	0.004	0.005	0.011	0.042	0.076	0.037	0.007	0.019
N3	0.006	0.072	0.129	0.045	0.095	0.064	0.030	0.048	0.271
N4	0.085	0.140	0.082	0.018	0.070	0.175	0.043	0.108	0.052
C5	0.002	0.065	0.044	0.050	0.013	0.024	0.010	0.028	0.090
N6	0.023	0.030	0.043	0.087	0.117	0.017	0.032	0.032	0.008
N7	0.123	0.093	0.228	0.123	0.089	0.125	0.147	0.098	0.011
C8	0.088	0.074	0.055	0.171	0.136	0.027	0.056	0.059	0.001
C9	0.038	0.026	0.022	0.036	0.019	0.011	0.036	0.031	0.001
C10	0.026	0.024	0.014	0.070	0.051	0.015	0.004	0.002	0.000
C11	0.039	0.030	0.025	0.058	0.036	0.009	0.090	0.077	0.002
C12	0.000	0.000	0.002	0.002	0.002	0.000	0.070	0.058	0.001
C13	0.045	0.034	0.034	0.071	0.050	0.014	0.075	0.067	0.002
C14	0.000	0.011	0.012	0.001	0.007	0.037	0.006	0.005	0.091
C15	0.001	0.009	0.016	0.001	0.012	0.047	0.006	0.007	0.081
C16	0.000	0.000	0.001	0.000	0.000	0.000	0.000	0.000	0.007
C17	0.001	0.005	0.011	0.002	0.015	0.071	0.009	0.010	0.142
C18	0.000	0.000	0.000	0.000	0.000	0.001	0.000	0.000	0.004
C19	0.001	0.003	0.010	0.002	0.013	0.049	0.006	0.006	0.082
X20[*1]	0.124	0.114	0.098	0.030	0.055	0.112	0.024	0.069	0.087
C21							0.011	0.010	0.000
C22							0.059	0.051	0.001
C23							0.012	0.009	0.000
C24							0.016	0.014	0.000

The numbers of atoms in the chemical structures are shown below.

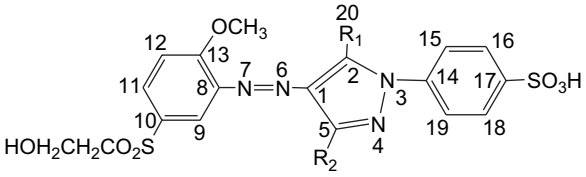

Pyr-Yellow (X^{*1}=N, $R_1 = NH_2$, $R_2 = CH_3$)
Carbopyr-Yellow (X^{*1}=O, R_1 = OH, R_2 = COOH)

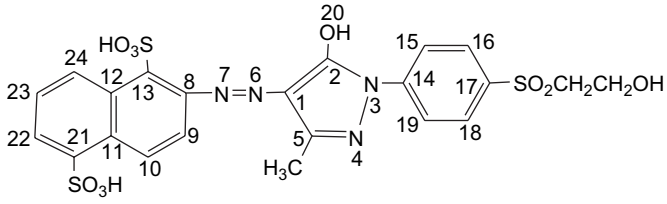

Naphpyr-Yellow

[2 + 2] cycloaddition between double bonds at different positions, although the values of $S^{(E)}_{m,n}$ showed some dominance between them, implying a limit to the analytical method using the heat of formation for the reaction intermediates.

For the reasons mentioned above, the authors adopted the other method to assess the ease of the two reactions, as first approximation, by comparing the heat of reactions for the corresponding reactions. Then, the reactivity to the two reactions may be discussed by the differences in the $\Delta_f H^\circ$(gas) of hydroperoxide for ene reaction and that for [2 + 2] cycloaddition product, 1,2-dioxetane. For the ATs of Pyr-Yellow, the order of the reactivity estimated by the heat of reactions was as follows:

$$\begin{aligned}&\text{ene (C1=C2; H(N20))} > \text{[2+2] cycloaddition (C1=C2)}\\ &> \text{[2+2] cycloaddition (C8=C13)}\\ &> \text{[2+2] cycloaddition (C8=C9)}\\ &> \text{ene (N4=C5; H(Me))}\\ &> \text{[2+2] cycloaddition (N4=C5)}\\ &> \text{[2+2] cycloaddition (C9=C10)}\\ &\gg \text{[2+2] cycloaddition (N6=N7)}\end{aligned} \quad (5)$$

Table 7
Heat of formation, $\Delta_f H^\circ$(gas) (kcal mol^{-1}), of intermediate and products in the ene and [2 + 2] cycloaddition reactions at the double bonds of (C1=N6), (C1=C2), (C1=C5) and (N4=C5) for the predominant tautomer of pyrazolinylazo dyes with singlet oxygen, calculated by PM5 method

	Tautomer	Molecular weight	$\Delta_f H^\circ$(gas) of intermediate at TSG[a]	$\Delta_f H^\circ$(gas) of intermediate	$\Delta_f H^\circ$(gas) of hydroperoxide	$\Delta_f H^\circ$(gas) of intermediate at TSG[a]	$\Delta_f H^\circ$(gas) of intermediate	$\Delta_f H^\circ$(gas) of addition product
Reaction mode (position)			Ene (C1=N6; H(N7))			[2 + 2] cycloaddition (C1=N6)		
Model pyrazolinylazo[*1]	HT	418.423	−8.344	−8.331	−54.479	−8.513	−8.439	−14.484
Yellow 13	HT	576.936	−214.313	−214.300	−264.608	−216.966	−216.966	−220.423
Yellow 14	HT	576.980	−175.829	−175.829	−219.760	−175.612	−175.609	−183.103
Yellow 17	HT	558.534	−200.467	−200.299	−242.155	−200.576	−200.510	−205.753
Yellow 2	HT	820.564	−225.703	−225.701	−268.476	−226.533	−226.532	−233.744
Carbopyr-Yellow	HT	558.491	−237.067	−237.045	−282.909	−238.353	−238.348	−244.788
Naphpyr-Yellow	HT	628.600	−219.962	−219.958	−266.830	−219.285	−219.279	−224.414
Reaction mode (position)			Ene (C1=C2; H(N20)			[2 + 2] cycloaddition (C1=C2)		
Model Pyr-Yellow[*2]	AT	497.497	−79.354[*3]	−79.354[*4]	−119.940[*5]	−79.182	−79.182	−109.967
Pyr-Yellow	AT	527.523	−115.701	−115.691	−157.290	−116.154	−116.154	−145.497
Reaction mode (position)			Ene (C1=C5; H(Me))			[2 + 2] cycloaddition (C1=C5)		
Yellow 13	A/KT	576.936	−214.687	−214.685	−256.854	−214.762	−214.762	−246.848
Yellow 2	A/KT	820.564	−221.037	−221.009	−262.980	−224.248	−224.191	−252.939
Naphpyr-Yellow	A/KT	628.600	−214.011	−213.913	−258.440	−213.307	−213.307	−247.048
Reaction mode (position)			Ene (N4=C5; H(Me))			[2 + 2] cycloaddition (N4=C5)		
Model pyrazolinylazo[*1]	HT	418.423	0.461[*6]	0.462[*7]	−36.414[*5]	0.490	0.461	−21.134
Yellow 13	HT	576.936	−214.728	−214.727	−243.789	−215.117	−214.990	−227.239
Yellow 14	HT	576.980	−173.161	−173.161	−218.439	−175.723	−175.665	−188.650
Yellow 17	HT	558.534	−200.647	−200.642	−226.787	−200.429	−200.427	−212.986
Yellow 2	HT	820.564	−224.335	−224.229	−253.076	−221.629	−221.607	−238.155
Carbopyr-Yellow	HT	558.491	–	–	–	−237.034	−236.997	−249.131
Naphpyr-Yellow	HT	628.600	−220.770	−220.764	−246.152	−218.222	−218.212	−231.772
Model Pyr-Yellow[*2]	AT	497.497	−78.894	−78.864	−99.606	−78.101	−78.092	−84.992
Pyr-Yellow	AT	527.523	−115.603	−115.568	−135.923	−115.603	−115.568	−122.571

In Scheme 1, starting material = (**1**)[*2], intermediate at TSG = (**2**)[*3], intermediate at PM5 geometry = (**2**)[*4] and the hydroperoxide = (**3**)[*5]. In Scheme 2, starting material = (**1**) [*1], intermediate at TSG = (**2**)[*6], intermediate at PM5 geometry = (**2**)[*7] and the hydroperoxide = (**3**)[*5].

[a] TSG = Transition state geometry.

Table 8
Heat of formation, $\Delta_f H^\circ$(gas) (kcal mol^{-1}), of intermediate and products (1,2-dioxetane) in [2 + 2] cycloaddition reactions at the double bonds of (C8═C9), (C8═C13), (C9═C10), (N6═N7), (C12═C13) and (C1═C5) for predominant tautomers of pyrazolinylazo dyes with singlet oxygen

Dye		Molecular weight	$\Delta_f H^\circ$(gas) of intermediate at TSG	$\Delta_f H^\circ$(gas) of intermediate	$\Delta_f H^\circ$(gas) of addition product
Reaction mode (position)			[2 + 2] cycloaddition (C8═C9)		
Pyr-Yellow	AT	527.523	−116.036	−115.924	−137.696
Yellow 17	HT	558.534	−200.581	−200.547	−220.546
Yellow 2	HT	820.564	−223.504	−223.483	−245.677
Carbopyr-Yellow	HT	558.491	−237.260	−237.231	−258.123
Yellow 13	A/KT	576.936	−214.578	−214.578	−232.873
Yellow 2	A/KT	820.564	−221.857	−221.856	−239.869
Naphpyr-Yellow	A/KT	628.600	−216.258	−216.257	−227.765
Reaction mode (position)			[2 + 2] cycloaddition (C8═C13)		
Pyr-Yellow	AT	527.523	−116.136	−116.114	−138.229
Yellow 14	HT	576.980	−175.769	−175.730	−197.589
Yellow 17	HT	558.534	−200.630	−200.630	−223.325
Carbopyr-Yellow	HT	558.491	−232.058	−232.988	−249.906
Naphpyr-Yellow	HT	628.600	−219.538	−219.530	−237.708
Yellow 13	A/KT	576.936	−215.849	−215.849	−224.140
Yellow 2	A/KT	820.564	−221.495	−221.495	−231.862
Naphpyr-Yellow	A/KT	628.600	−213.422	−216.313	−239.047
Reaction mode (position)			[2 + 2] cycloaddition (C9═C10)		
Pyr-Yellow	AT	527.523	−116.172	−116.060	−121.166
Yellow 17	HT	558.534	−200.521	−200.468	−225.357
Carbopyr-Yellow	HT	558.491	−237.351	−237.347	−242.752
Reaction mode (position)			[2 + 2] cycloaddition (N6═N7)		
Pyr-Yellow	AT	527.523	−116.106	−116.033	−98.956
Yellow 13	A/KT	576.936	−214.708	−214.704	−198.463
Yellow 2	A/KT	820.564	−224.498	−224.498	−202.971
Naphpyr-Yellow	A/KT	628.600	−217.913	−217.905	−197.598
Reaction mode (position)			[2 + 2] cycloaddition (C12═C13)		
Yellow 13	A/KT	576.936	−215.660	−215.604	−225.561
Yellow 2	A/KT	820.564	−221.496	−221.494	−227.965
Reaction mode (position)			[2 + 2] cycloaddition (C1═C5)		
Yellow 2	A/KT	820.564	−224.373	−224.369	−252.939

Table 9
Heat of formation, $\Delta_f H^\circ$(gas) (kcal mol^{-1}), of intermediates and products (1,2-dioxetane) in the [2 + 2] cycloaddition reactions at the possible double bonds of (C14═C15), (C14═C19), (C16═C17), (C17═C18), (C10═C11) and (C11═C12) for the predominant tautomer of dyes with singlet oxygen

	M.W.	$\Delta_f H^\circ$(gas) of intermediate at TSG	$\Delta_f H^\circ$(gas) of intermediate	$\Delta_f H^\circ$(gas) of hydroperoxide	$\Delta_f H^\circ$(gas) of intermediate at TSG	$\Delta_f H^\circ$(gas) of intermediate	$\Delta_f H^\circ$(gas) of addition product
Mode		[2 + 2] cycloaddition (C14═C15) for HT			[2 + 2] cycloaddition (C14═C19) for HT		
Yellow 13	576.936	−216.808	−216.771	−235.283	−216.808	−216.771	−235.283
Yellow 14	576.980	−175.862	−175.860	−193.685	−175.945	−175.939	−193.942
Yellow 17	558.534	−200.539	−200.535	−218.949	−200.515	−200.512	−218.949
Yellow 2	820.564	−224.329	−224.318	−243.410	−224.353	−224.342	−242.275
Carbpyr-Yellow	558.491	−236.813	−236.813	−255.555	−236.813	−236.813	−255.555
Naphpyr-Yellow	628.600	−219.391	−219.389	−238.430	−219.391	−219.389	−238.430
Mode		[2 + 2] cycloaddition (C16═C17) for HT			[2 + 2] cycloaddition (C17═C18) for HT		
Yellow 14	576.980	−175.733	−175.713	−182.414	−175.779	−175.777	−182.402
Yellow 2	820.564	−224.170	−224.165	−235.721	−222.854	−222.849	−233.676
Mode		[2 + 2] cycloaddition (C10═C11) for HT			[2 + 2] cycloaddition (C11═C12) for HT		
Yellow 17	558.534	−200.603	−200.550	−208.288	−200.928	−202.920	−214.766
Yellow 2	820.564	−223.551	−223.516	−238.245	−223.550	−223.550	−240.739
Mode		[2 + 2] cycloaddition (C10═C11) for A/KT			[2 + 2] cycloaddition (C11═C12) for A/KT		
Yellow 2	820.564	−213.373	−213.356	−239.287	−221.459	−221.418	−241.026
Naphpyr-Yellow	628.600	–	–	–	−213.373	−213.356	−220.814

MO calculation implies that both the ene and [2 + 2] cycloaddition reactions may occur at the double bonds of C1=C2 and N4=C5 in pyrazoline ring, although the reactions take place more predominantly at the double bond of C1=C2 than that of N4=C5 (cf. Table 7). The possibility of reactions other than ene (C1=C2; H(N20)) may be reduced due to the low heat of reaction for the reaction modes, resulting in the predominant mode of reaction illustrated in Scheme 1(a). For the next probable reaction mode, [2 + 2] cycloaddition (C1=C2), the reaction scheme may be described as shown in Scheme 1(b), resulting in the same decomposed product bound with cellulose as that of the ene reaction. If the next probable mode occurred, no confirmation of the contribution may be possible. This fact may indicate no exclusion of the possibility of reaction at the other double bonds. Although the contribution of individual double bonds to the reactivity may be small enough, the summation of their contributions becomes considerably large. The $\Delta_f H^\circ$(gas) values for (C8=C9) might indicate also some contribution of this bond due to the double bond character, since no double bond was fixed in benzene ring. In this case, no double counting of $S^{(E)}_{m,n}$-values must be made.

Judging only from $S^{(E)}_{m,n}$ values, the double bond of N6=N7 may have high potential reactivity. However, Table 8 showed that the $\Delta_f H^\circ$(gas) values for the products are higher than those for the products at the other double bonds, implying that the reaction may not proceed at the intermediate stage. As explained below, four dyes among seven dyes examined have azo groups with high reactivity (cf. Table 8). Since $S^{(E)}_{m,n}$ (m,n: 6,7) for these dyes are too large to neglect, the exclusion of the bond from reactivity results in the considerable deviations of their plots from the common correlation line (cf. Fig. 5). The energy barrier of dioxetanes from azo group may be regarded to be overcome by the high energies of singlet oxygen.

Besides the double bond of N6=N7, the exclusion of the reactivity of N4=C5 may be explained as follows: in the MO calculation of $\Delta_f H^\circ$(gas) for ene (N4=C5; H(Me)) and [2 + 2] cycloaddition (N4=C5), the reaction intermediates may be constructed by shifting electron density to bind the oxygen with carbon (C5) in spite of the very small d_{HOMO}, while the values of d_{HOMO} and $f_r^{(E)}$ may describe the values before the binding.

According to Scheme 1(a), azo scission may result in 2-methoxy-5-(2-hydroxyethyl-sulfonyl)phenol bound with cellulose as one of the main end products, although the details of the reaction scheme of group transformation after the ene intermediate to form the corresponding hydroperoxide as well as 1,2-dioxetanes via [2 + 2] cycloaddition and their thermal decomposition were not sought [8,11,21,51–69]. Since the [2 + 2] cycloaddition (C8=C13) may cause the bond scission of C8–N7 and the [2 + 2] cycloaddition (C9=C10) that of C10–sulfur as the side reactions (cf. Section 3.6.2.1), their reactions may result in the fading of dyes on cellulose. The decomposed product may be a phenyl residue with a VS anchor and a VS anchor without an aromatic nucleus. The existence of the ene product in the absorption spectrum may prove the validity of the primary mechanism analysed. The same shape of the spectra for the end products as that of Yellow 14 (cf. Section 3.6.2.2) may indicate its validity.

Plotting the $S^{(E)}_{m,n}$ value for the corresponding atomic positions of double bonds that have the possibility of reacting with singlet oxygen against $\log k_0$, at first for the most reactive position and secondly adding the contribution of following reactive ones, is illustrated in Fig. 5. Taking the plots of all the dyes examined into consideration produced a linear correlation between $S^{(E)}_{m,n}$ values vs. $\log k_0$. The plot of the $S^{(E)}_{m,n}$ (m,n: 1,2, 6–10,13) value for ene (C1=C2; H(N20)) and/or [2 + 2] cycloaddition of the corresponding bonds for the ATs fitted with the linear correlation line between the $S^{(E)}_{m,n}$ value vs. $\log k_0$ for a series of azo dyes examined. The addition of the contribution of ene (N4=C5; H(Me)) and/or [2 + 2] cycloaddition (N4=C5) caused sideward deviation from the line of correlation, while the exclusion of [2 + 2] cycloaddition (N6=N7) resulted in a deviation in the reverse direction.

3.6.2. Reaction of azo dyes with same diazo component as that of Pyr-Yellow

3.6.2.1. HTs for model pyrazolinylazo dyes. Pyrazolinylazo dyes with an *o*-hydroxy group may exist predominantly as the HTs in the gas phase except for Pyr-Yellow with an *o*-amino group. (The chemical structure of a model compound (**1**) used for the explanation is illustrated in Scheme 2. $\Delta_f H^\circ$(gas) for the ATs = -22.916 kcal mol^{-1} and that for the HTs = -32.069 kcal mol^{-1}.) The reaction scheme for the HTs is described in Scheme 2(a) for ene (N4=C5; H(Me), and 2(b) for [2 + 2] cycloaddition (N4=C5) as the HTs of a model compound. The schemes of each reaction mode for each dye examined may be explained by this scheme, although a modification of substituents is needed.

3.6.2.2. HTs of Yellow 14 and Carbopyr-Yellow. Yellow 14, Pyr-Yellow and Carbopyr-Yellow belong to this group of dyes (Group A). The spectra of the decomposed products for the three dyes, illustrated in Fig. 2, coincided with each other, although those for Carbopyr-Yellow showed some deviations and remain debatable. Yellow 14 and Carbopyr-Yellow may exist as

HTs. The d_{HOMO} for Yellow 14 in Table 5 suggests that the double bonds with probable reactivity were C1=N6 and N4=C5 in pyrazoline ring, the bonds around C14 and C17 in *N*-phenyl ring and those around C8 in diazo component. The other double bonds around had also some reactivity. In the case of Carbopyr-Yellow (cf. Table 6), the reactivity of C1=N6 may be excluded due to the small value of d_{HOMO} at N6, that around C17 due to the small one at C16 and C18 and that around C10 due to the small one at C9. The exclusion of the reactivity for Yellow 14 is fewer than that of Carbopyr-Yellow (cf. Table 2). That is why Carbopyr-Yellow has smaller reactivity than Yellow 14 in spite of their similar properties. These double bonds have a possibility of performing the ene and [2 + 2] cycloaddition reactions. Only the reaction scheme of the latter mode for HTs is illustrated in Scheme 2(b), but the schemes for the other modes may be seen by the analogy to the illustrated ones. The four reaction modes, ene (C1=N6; H(N7) and N4=C5; H(Me)), [2 + 2] cycloaddition (C1=N6 and N4=C5), might result in a common decomposed product of the diazo component, 2-methoxy-5-(2-hydroxyethylsulfonyl)phenol. But no one could decide which modes of reaction occurred from the absorption spectra of the decomposed products. The λ_{max} of the absorption spectra of completely decomposed products for Pyr-Yellow and Yellow 14 (cf. Fig. 2(a) and (b)) were 202.5 and 242.5 nm (relative ratios = 1.0:0.60 for Pyr-Yellow and 1.0:0.58 for Yellow 14), a complete coincidence of the spectra.

The results of enthalpy analyses for the end products, hydroperoxide and dioxetane, of the nine reaction modes of Yellow 14 and Carbopyr-Yellow are listed in Tables 7 and 8. Carbopyr-Yellow has no possibility of an ene reaction at N4=C5 due to the lack of a hydrogen atom to be abstracted. The heat of reaction estimated from the values of $\Delta_f H^\circ$(gas) for the HTs of Carbopyr-Yellow in the seven modes of reaction indicated the reactivity in the following order:

ene (C1=N6; H(N7))
$\gg$ [2+2] cycloaddition (C14=C15)
$=$ [2+2] cycloaddition (C14=C19)
$>$ [2+2] cycloaddition (C8=C13)
$>$ [2+2] cycloaddition (N4=C5)
$>$ [2+2] cycloaddition (C1=N6)
$>$ [2+2] cycloaddition (C9=C10) (6)

The order of reactivity from the $S^{(E)}_{m,n}$ values listed in Table 3 was very different from that of (6). The $S^{(E)}_{m,n}$ values indicated the dominant reactivity of N4=C5 and the following reactivities at several double bonds as listed in Table 3. For the same reason (smaller values of $f^{(E)}_r$ at both sites than at N6), the reactivity at C9=C10 may be excluded. In the MO calculation of $\Delta_f H^\circ$(gas) for ene (C1=N6; H(N7)), the reaction intermediate may be constructed by shifting electron density to bind the oxygen with the nitrogen (N6). The values of d_{HOMO} and $f^{(E)}_r$ may describe the values before the binding. The order of reactivity was estimated from the $S^{(E)}_{m,n}$ values by taking also the order from the $\Delta_f H^\circ$(gas) values of the reaction intermediates and the products into consideration.

On the other hand, the heat of reaction estimated similarly by the nine modes of reaction (cf. Table 3) indicated the following order of reactivity for the HTs of Yellow 14:

ene (C1=N6; H(N7)) $>$ ene (N4=C5; H(Me))
$>$ [2+2] cycloaddition (C8=C13)
$>$ [2+2] cycloaddition (C14=C19)
$\approx$ [2+2] cycloaddition (C14=C15)
$>$ [2+2] cycloaddition (N4=C5)
$>$ [2+2] cycloaddition (C1=N6)
$>$ [2+2] cycloaddition (C16=C17)
$\approx$ [2+2] cycloaddition (C17=C18) (7)

Differences among reaction modes in the heat of reaction were small, although a small difference between the double bonds of different positions was noticed. The $S^{(E)}_{m,n}$ value at the atomic position of the double bonds, listed in Table 2, also indicated considerably higher reactivity of N4=C5 than that of C1=N6. Both the enthalpy analyses and the treatment by frontier orbital theory on the probable reaction modes for Yellow 14 indicated that the reaction occurred primarily at both the double bonds of C4=C5 and C1=N6 and secondarily in the double bonds around atoms bound with large substituents.

The absorption spectra of decomposed products for Carbopyr-Yellow showed some resemblance in the shape. The λ_{max} of the spectra for this dye (cf. Fig. 2(c)) were 202.5 and 242.5 nm (relative ratios = 1.0:0.71), a complete coincidence in the wavelength for Pyr-Yellow and Yellow 14 but some differences in the ratio.

The plot of $S^{(E)}_{m,n}$ value (*m*,*n*: 1,4–6, 8,13–19) for Yellow 14 and that of the $S^{(E)}_{m,n}$ value (*m*,*n*: 4,5,8,13–15,19) for Carbopyr-Yellow against $\log k_0$ fit well the linear common correlation together with other dyes. The fitness of the plots for the HTs of two dyes was good with the common correlation line drawn in Fig. 5, as well as the accordance of the absorption spectra of the decomposed products, suggesting that the above discussions on the AHT by $\Delta_f H^\circ$(gas) and $\Delta_f H^\circ(H_2O)$ and the reactivity using frontier orbital theory were consistent with the experiments.

3.6.3. Reaction of pyrazolinylazo dyes that contain VS anchor in coupling component

3.6.3.1. HTs of Yellow 13 and Naphpyr-Yellow. Yellow 13 and Naphpyr-Yellow, synthesized with the same coupling component, which possesses a VS anchor, belong to this group (Group B). Yellow 13 may exist dominantly as HTs with a considerable population as A/KTs in the gas phase, while predominantly as A/KTs in water. Naphpyr-Yellow may exist as HTs in the gas phase and as A/KTs in water.

The estimated values of $\Delta_f H^\circ$(gas) for the end products of Yellow 13 in the six modes of reactions indicated similarly the reactivity in the following order:

$$\begin{aligned}&\text{ene(C1=N6; H(N7))} \gg \text{ene(N4=C5; H(Me))}\\ &> [2+2]\ \text{cycloaddition (C14=C15)}\\ &= [2+2]\ \text{cycloaddition (C14=C19)}\\ &> [2+2]\ \text{cycloaddition (C1=N6)}\\ &> [2+2]\ \text{cycloaddition (N4=C5)}\end{aligned} \quad (8)$$

and those for the end products of Naphpyr-Yellow for the seven modes of reactions are in the following order:

$$\begin{aligned}&\text{ene (C1=N6; H(N7))} \gg \text{ene (N4=C5; H(Me))}\\ &> [2+2]\ \text{cycloaddition (C14=C15)}\\ &= [2+2]\ \text{cycloaddition (C14=C19)}\\ &> [2+2]\ \text{cycloaddition (C8=C13)}\\ &> [2+2]\ \text{cycloaddition (N4=C5)}\\ &> [2+2]\ \text{cycloaddition (C1=N6)}\end{aligned} \quad (9)$$

The reaction of two dyes with singlet oxygen may occur dominantly at the double bonds of C1=N6 and N4=C5, but the $f_r^{(E)}$ values listed in Tables 2 and 3 indicated clearly the predominance of the latter double bond. Although the chemical structures of the chromophores are different, the reaction schemes are illustrated in Scheme 2(a) for ene (N4=C5), and (b) for [2 + 2] cycloaddition (N4=C5). The schemes for the other modes may be seen by analogy of the illustrated ones.

In the case of Yellow 13, the $S_{m,n}^{(E)}$ (m,n: 1,6) value may be excluded due to the small values of d_{HOMO} at C1 (0.007) and N6 (0.01), respectively, as well as the $f_r^{(E)}$ values as listed in Table 2. The reactivities at the double bonds of C16=C17, C17=C18 and C18=C19 may be also excluded due to the small values of d_{HOMO} at the alternating positions, C16 (0.005) and C18 (0.005) in spite of large values of $f_r^{(E)}$ and d_{HOMO} at C17 and C19. The exclusion may lower the reactivity of the HTs.

The plot of $S_{m,n}^{(E)}$ (m,n: 4,5,14,15,19) for the HTs of Yellow 13 vs. $\log k_0$ showed a deviation from the common correlation line in the direction of smaller reactivity.

On the other hand, the $f_r^{(E)}$ values at the double bond of C8=C13 for the HTs of Naphpyr-Yellow in Table 3 at 0.046 (C8) and 0.055 (C13) were not small, while the values of d_{HOMO} (0.001 (C8) and 0.002 (C13)) were extremely small in spite of the $f_r^{(E)}$ values. The sum, $S_{m,n}^{(E)}$ (m,n:8,13), was small compared with the values for other dyes exhibiting reactivity, indicating a limit of reactivity. (As mentioned above, the reactivity at the double bond with such small values of d_{HOMO} was regarded as negligible.) If the contribution of this position was taken into consideration, the plots of $S_{m,n}^{(E)}$ (m,n:4,5,14,15,19) vs. $\log k_0$ showed a deviation from the correlation line, but ignoring this bond gave a good coincidence as the HTs. Although the limiting value to the reactions with singlet oxygen could not be determined experimentally or from the absorption spectra of decomposed products, the assumption regarding negligibility may be supported. Since the contribution of the reaction at the double bond of C8=C13 may be ignored as described above, the reaction scheme was not illustrated.

When the reaction scheme for [2 + 2] cycloaddition (N4=C5) was considered, the decomposed product for these two dyes, 4-(2-hydroxyethylsulfonyl)-2-nitrosoaniline, might be identical (cf. Scheme 2(b)). The absorption spectra of decomposed products for Yellow 13 and Naphpyr-Yellow were very similar to each other, a further resemblance between them; compared with that between dyes of Group A. Inspecting the spectra in detail, however, Yellow 13 had a tiny absorption peak around 350 nm unlike Naphpyr-Yellow, while the latter dye had a small peak around 220 nm. Since the other parts of the spectra or the general pattern resembled each other, complete solution might be impossible. Prolonged exposure of Yellow 13 seemed to decrease the absorption around 350 nm, which probably explains an incomplete group transformation due to a short time of exposure to Yellow 13 resulting in a mixture of compounds (**3**) as shown in Scheme 2(a) and (b), or a co-occurrence of the reaction at C1=N6 to the reaction products due to the reactions at N4=C5. In fact, since many possibilities could occur, the complete analysis might be impossible. However, the resemblance in the spectral shape might indicate the existence of common reaction schemes.

The plot of the $S_{m,n}^{(E)}$ (m,n:4,5,14,15,19) value for the HTs of Naphpyr-Yellow vs. $\log k_0$ fit considerably well into the linear correlation among all the dyes examined, as mentioned above, while that for the HTs of Yellow 13 showed some deviations in the lower direction from the linear relation.

Incoherence between the $S_{m,n}^{(E)}$ values and the inequality (8) in the reactivity might imply that the reactions at C1=N6 required a large activation energy or a large modification of molecular geometry to cause the double bond and singlet oxygen to interact for both the dyes. The $S_{m,n}^{(E)}$ values might describe the reactivity of

the double bond before reaction, while the energy of formation for the product and even for the intermediate might describe the reactivity after reaction or at the geometry of the intermediate.

3.6.3.2. A/KTs of Yellow 13 and Naphpyr-Yellow. Unlike Pyr-Yellow and Yellow 14, the HTs of Yellow 13 decreased the stability with a transfer from the gas phase into water, resulting in the HTs as the predominant tautomer but with a considerable population as the A/KTs in the gas phase. As a comparison, the A/KTs of Naphpyr-Yellow exhibiting similar AHT were also analysed. The reaction modes and their reactivities were tried to discuss them as the minor contributions to the HTs. No MO parameters useful for describing the reactivity of the A/KTs on cellulose might be available, since the A/KTs in the gas phase possessed lower stability than the HTs.

From the $\Delta_f H^\circ$(gas) values of the end products for probable reaction modes, the order of reactivity of the A/KTs for Yellow 13 was as follows:

$$\begin{aligned}&\text{ene(C1=C5; H(Me))} > \text{[2+2] cycloaddition (C1=C5)}\\ &> \text{[2+2] cycloaddition (C8=C9)}\\ &> \text{[2+2] cycloaddition (C12=C13)}\\ &> \text{[2+2] cycloaddition (C8=C13)}\\ &\gg \text{[2+2] cycloaddition (N6=N7),}\end{aligned} \tag{10}$$

and the order of reactivity of the A/KTs for Naphpyr-Yellow was as follows:

$$\begin{aligned}&\text{ene(C1=C5; H(Me))} > \text{[2+2] cycloaddition (C1=C5)}\\ &> \text{[2+2] cycloaddition (C8=C13)}\\ &> \text{[2+2] cycloaddition (C8=C9)}\\ &> \text{[2+2] cycloaddition (C11=C12)}\\ &> \text{[2+2] cycloaddition (N6=N7).}\end{aligned} \tag{11}$$

The orders (10) and (11) were almost the same for both the dyes. The $S^{(E)}_{m,n}$ values at different double bonds indicated a different order: the amino-substituted carbon atom of the diazo component had the greatest reactivity. $S^{(E)}_{m,n}$ (*m*,*n*:8,9) for Yellow 13 and $S^{(E)}_{m,n}$ (*m*,*n*: 8,13) for Naphpyr-Yellow were estimated to be the unique probable double bonds of the reaction. The next predominant double bond (N4=C5) seemed to contribute to the reactivity of Yellow 13, but almost not for Naphpyr-Yellow. The contributions of the double bonds of C8=C13 and C12=C13 for Yellow 13 may contribute to the reactivity of A/KTs for Yellow 13. However, the contribution of C2 and N4 may be excluded due to the lack of double bond at C1=C2 and N4=C5 in spite of large values of $f^{(E)}_r$ at C2 and N4, listed in Table 2. The validity of these selections could not be examined experimentally. The plot of $S^{(E)}_{m,n}$ (*m*,*n*:1,5–8,11–13) for the A/KTs of Naphpyr-Yellow vs. $\log k_0$ showed a very large deviation in the higher direction.

As shown in Table 2 for the $f^{(E)}_r$ value and in Table 5 for d_{HOMO}, the double bonds with predominant reactivity varied with tautomers due to the shifts of electrons of HOMO. The reactivities, however, were treated as similar to each other. The $S^{(E)}_{m,n}$ (*m*,*n*: 1,2,4–9,12,13) value for the predominantly reactive positions for the A/KTs of Yellow 13 showed a slight deviation from the common correlation line between the $S^{(E)}_{m,n}$ value and $\log k_0$ for all the dyes in the larger direction of reactivity (Fig. 5). Thus, an intermediate point between $S^{(E)}_{m,n}$ (*m*,*n*: 1,2,4–9,12,13) of the A/KTs and $S^{(E)}_{m,n}$ (*m*,*n*:4,5,14,15,19) for the HTs coincided with the common correlation line of all the dyes examined, as expected, although the populations of HTs and A/KTs for Yellow 13 could not be determined. The contributions of both tautomers resulted in a good fit with the common line of correlation for this dye.

Compared the reactivity of this dye with those of the other dyes, Yellow 13 had rather low reactivity; the values of $f^{(E)}_r$ (Table 2) and d_{HOMO} (Table 5) of this dye were smaller than those of the other dyes, resulting in a lack of reactivity at some double bonds. The transfer from the A/KTs to the HTs seemed to strengthen the tendency such as a lack of reactivity at C8.

In the case of A/KTs for Naphpyr-Yellow, the plot of the $S^{(E)}_{m,n}$ (*m*,*n*:1,5,6–8,11–13) value vs. $\log k_0$ deviated markedly in the larger direction, a shift from the correlation line. The contributions of the double bond at (C1=C2) for this dye may be excluded due to the small values of $f^{(E)}_r$ (0.014) and of d_{HOMO} (0.007) at C2, while the contribution at N4=C5 due to the lack of double bond of N4=C5. If the small deviation in the lower direction for the HTs was taken into consideration, the reactivity of this dye may be described by the present treatment irrespective of the large deviations of the A/KTs.

Since reactions at N4=C5 may result in ring opening to give a pyrazoline residue and those at the latter positions may give the original coupling component or its 4-substituted compound, the decomposed products may be a mixture of these products. The absorption spectra of the decomposed products would be identical if only the original component was formed. Because this might not be the case, the spectra might resemble each other but not be the same. The absorption spectra illustrated in Fig. 2(a) and (b) seem to show these situations accurately. Unfortunately, however, further analyses to confirm the validity of above discussion may be impossible.

3.6.4. Reaction of HTs for Yellow 17

This dye may exist predominantly as HTs in both the gas phase and water. No differences in the reaction modes and the absorption spectra of decomposed

products, except for the effects by 5-methoxy group, therefore, from those of Group A may be anticipated.

The heats of formation for the end products of each reaction mode indicated the reactivity in the following order:

ene (C1═N6; H(N7)) > ene (N4═C5; H(Me))
> [2+2] cycloaddition (C9═C10)
> [2+2] cycloaddition (C8═C13)
> [2+2] cycloaddition (C8═C9)
> [2+2] cycloaddition (C14═C15)
= [2+2] cycloaddition (C14═C19)
> [2+2] cycloaddition (C11═C12)
> [2+2] cycloaddition (N4═C5)
> [2+2] cycloaddition (C1═N6) (12)

The distribution of d_{HOMO} for HTs as well as the $f_r^{(E)}$ values suggested higher reactivity at the double bond of (C8═C13) than at the double bond of (N4═C5), although the inequality (12) did not show the same order. The sum of $f_r^{(E)}$ values at the atomic positions of the double bonds, listed in Tables 2 and 3, also indicated considerable reactivities at the double bonds around C8, C14 and C11 from the lower limits of the $S_{m,n}^{(E)}$ as in the case of Yellow 14.

Taking the inequality (12) and the $f_r^{(E)}$ values in Table 3 into consideration, [2 + 2] cycloaddition (C8═C13), ene (N4═C5; H(Me)) and [2 + 2] cycloaddition (N4═C5) may occur dominantly. The reaction scheme of ene (N4═C5; H(Me)) is described in Scheme 2(a) and that of [2 + 2] cycloaddition (N4═C5) in Scheme 2(b), although anchor groups as well as two methoxy groups are not included in the schemes. The schemes for the other modes may be seen by analogy to the illustrated ones.

Therefore, the reaction schemes for Yellow 17 may be the same as those for Group A at the double bond of N4═C5 and different from them at C8═C9 and partially similar at the reaction at C1. Like Group A, the absorption spectra of decomposed products that were generated via the two modes of reaction might be the same as each other. A peak around 300 nm might be attributed to incomplete group transformation due to the shorter period of exposure to Yellow 17.

Plotting the $S_{m,n}^{(E)}$ (m,n: 4,5,8−15,19) values of this dye against $\log k_0$ obtained above, whose positions were mentioned from the above analyses, produced a good fit with the linear correlation for all the dyes (Fig. 5). The position of C1═N6 may be excluded due to the very small value of $f_r^{(E)}$, 0.014 (N = 6). The decomposed products may be supposed to be a mixture of 1-substituted 2,5-dimethoxy-4-(2-hydroxyethylsulfonyl)-phenol and the absorption spectra may not contradict the above discussion.

3.6.5. Reaction of Yellow 2

The heats of formation in both the gas phase and water indicated that this dye exists predominantly as HTs in water and in a mixture of HTs and A/KTs in the gas phase. The reactivity of this dye is analysed for HTs and A/KTs.

3.6.5.1. HTs. From the distribution of d_{HOMO} and the $f_r^{(E)}$ values for the HTs, almost double bonds may possess a possibility of reacting. The heats of formation of the end products for Yellow 2 in the twelve modes of reaction indicated reactivity in the following order:

ene (C1═N6; H(N7)) ≫ ene (N4═C5; H(Me))
≈ [2+2] cycloaddition(C1═C5)
> [2+2] cycloaddition (C8═C9)
> [2+2] cycloaddition (C14═C15)
≈ [2+2] cycloaddition (C14═C19)
> [2+2] cycloaddition (C11═C12)
> [2+2] cycloaddition (N4═C5)
= [2+2] cycloaddition (C10═C11)
> [2+2] cycloaddition (C16═C17)
> [2+2] cycloaddition (C17═C18)
= [2+2] cycloaddition (C1═N6) (13)

The order of reactivity from the $S_{m,n}^{(E)}$ values was difficult to compare with the order (13). The ene at the double bond of C10═C11 was excluded due to the lack of an active hydrogen to be abstracted. The reactions at the double bond of C10═C11 might be excluded due to the very small values of $f_r^{(E)}$ values at C10 and that of C1═N6 as in the boundary. The reactivity at N7 may be excluded due to the lack of double bond around N7 irrespective of considerable value of $f_r^{(E)}$ (Table 3). Taking the inequality (13) and the $f_r^{(E)}$ values in Table 3 into consideration, the reactivity of HTs was analysed.

Among the possible modes of reaction, only the reaction schemes of ene (N4═C5; H(Me)) and [2 + 2] cycloaddition (N4═C5) are described in Scheme 2(a) and (b), although the substituents including anchors should be modified. The schemes for the other modes may be seen by analogy to the illustrated ones.

According to Scheme 2(a) and by analogy, the decomposed products combined with cellulose may be identical irrespective of the modes and sites of reaction, while in [2 + 2] cycloaddition (C11═C12) the 3-sulfoanilino ring may be opened. Whether or not all the modes or either one or two of them occurred may not be determined from the absorption spectra of decomposed products.

Since superposition of two reaction modes at the same atomic position results in the occurrence of either mode, the sum of the $f_r^{(E)}$ values at several double

bonds may describe the whole reactivity of Yellow 2. Plotting the $S^{(E)}_{m,n}$ (m,n: 1,4–6,8,9,11–19) value against $\log k_0$ showed a large shift sideward in the lower direction to the common correlation line among all dyes examined.

3.6.5.2. A/KTs. As Table 3 shows, Yellow 2 has the possibility of existing as a mixture of HTs and A/KTs on cellulose. No precise population ratio of these two tautomers could be estimated, although the HTs might be predominant over the A/KTs. From the distribution of d_{HOMO} and the $f^{(E)}_r$ values for the HTs, six double bonds, C1=C5, C8=C9, C10=C11, C12=C13, C8=C13 and N6=N7, may possess the possibility of reacting. The reactivity related to C2 and C14 was considerably lowered by the substituent effects due to the very small values of $f^{(E)}_r$ at C2 and C14, compared with those of HTs.

The heats of formation of the end products for Yellow 2 in the five modes of reaction indicated the reactivity in the following order:

$$\begin{aligned}&\text{ene (C1=C5; H(Me))} > [2+2]\text{ cycloaddition (C1=C5)}\\ &> [2+2]\text{ cycloaddition (C11=C12)}\\ &> [2+2]\text{ cycloaddition (C8=C9)}\\ &\approx [2+2]\text{ cycloaddition (C10=C11)}\\ &> [2+2]\text{ cycloaddition (C8=C13)}\\ &> [2+2]\text{ cycloaddition (C12=C13)}\\ &> [2+2]\text{ cycloaddition (N6=N7)}\end{aligned} \quad (14)$$

The order of reactivity from the $S^{(E)}_{m,n}$ values (cf. Table 3) coincided well with the order (14). Plotting of the $S^{(E)}_{m,n}$ (m,n: 1,5–13) value against $\log k_0$ showed a large shift sideward in the smaller direction to the common correlation line among all dyes examined as in the case of HTs. However, the values of $S^{(E)}_{m,n}$ (m,n: 1,4–6,8–9,11–19) for the HTs and $S^{(E)}_{m,n}$ (m,n: 1,5–13) for A/KTs were almost identical with each other, an exceptional behavior in azo dyes was examined. It may be due to the lack of reactivity at C1=C2 and around C14 by the very small values of $f^{(E)}_r$ at C2 and C14, respectively, and due to that at N4=C5 by no double bond character in the A/KTs. The results obtained using MOPAC program of the present version seemed to give smaller values of d_{HOMO} and $f^{(E)}_r$ in the chromophore of this dye compared with the other dyes examined, because d_{HOMO} existed also in triazine ring.

Compared with the complexity of the reaction mechanism, the absorption spectra observed seemed to be simple. Although there might be no contradiction between them, no further discussion may be impossible.

3.7. Analyses of particular substituent effects

Among dyes examined, some particular effects improving the photostability were recognized.

3.7.1. Effect of o-sulfo groups on reactivity of azo dyes

Among the seven dyes, three dyes (Yellow 2, Yellow 13 and Naphpyr-Yellow) with relatively low reactivity toward singlet oxygen possess a sulfo group at the *o*-position to the amino group in the diazo component. No other substituents were recognized to decrease the reactivity against singlet oxygen. It was found to be difficult to elucidate the effect of *o*-sulfo groups on the reactivity of parent dyes because, for example, if all the substituents in the *N*-phenyl and diazo components were removed to simplify the effect, no definite effects of the *o*-sulfo group were clarified, since introducing *o*-sulfo groups changed the AHT. A decrease in the reactivity by the *o*-sulfo group may be attributed to compound effects caused by the mutual interactions of many factors.

As far as these three dyes are concerned, the introduction of *o*-sulfo groups decreased the d_{HOMO} at C1 (the position of coupling). Since, in HOMO, a decrease in d_{HOMO} at C1 may result inevitably in an increase at the other positions (total density = 1.0), *o*-sulfo groups did not always cause a decrease in the reactivity toward singlet oxygen. In fact, the *o*-sulfo groups of a model compound (1*N*-phenyl-3-methyl-4-phenylazopyrazol-5-one) decreased the d_{HOMO} at C8, but not at C1, compared with the original compound. Thus, in the three dyes examined, substituents other than the *o*-sulfo group might disperse electrons in HOMO so as to decrease the reactivities of double bonds in the total molecule. The detailed analyses of substituents in a particular dye on the photo reactivity may be a future theme in R&D in dye chemistry.

3.7.2. Effect of AHT and d_{HOMO} at particular atom on reactivity of dyes

Tables 2 and 3 show that only one dye existed dominantly as ATs in the gas phase, three dyes as HTs, and the other four dyes had, besides HTs, the contribution of A/KTs needed to take into consideration. Although electrons shifted by AHT, whether or not the reactivity against singlet oxygen changes with AHT is not determined without any qualification. But HTs in the four dyes listed had lower reactivity than that of ATs or A/KTs except for Yellow 2. Since the number of electrons in each orbital is constant, a reason why HTs had such properties must exist. Inspecting d_{HOMO} in Tables 5 and 6 indicated that the primary reason for low reactivity was the high d_{HOMO} at N3, a site of non-reactivity. Irrespective of the population of tautomers, except for Carbopyr-Yellow, high density at the nitrogen lowered indirectly the $f^{(E)}_r$ values in the sites

of reaction for the HTs of the six dyes. This property might be effective against singlet oxygen but not usually against electrophiles and sometimes against nucleophiles. The reactive dyes should be molecular-designed from various viewpoints, since in principle, there are no dyes with non-reactivity against all chemicals.

3.7.3. Relationship between light fastness on cotton and reactivity toward singlet oxygen

In previous studies [10,79], the authors found a linear relationship between the ratings of light fastness (LF) of reactive azo dyes as well as vat dyes on dry cotton fabrics and $\log(k_0 f)$, where f is the photosensitivity of the dye. Unfortunately, no f values of the seven yellow dyes were determined due to the spectral overlap on the spectrum of Pyr-Yellow, which has been used as a probe to determine the f values for a series of dyes other than yellow dyes. Since the f value of Pyr-Yellow was estimated to be very small [10], those for the other pyrazolinylazo dyes may be also small, as supposed by the fact that they have similar ratings of excellent perspiration-light fastness (Table 1).

The LF of dyes examined is listed in Table 1. If the factor of photosensitivity was assumed to be nearly constant, or was ignored, for all the yellow dyes examined, they showed a linear relation between $\log k_0$ and the ratings of LF. This fact implies that pyrazolinylazo dyes possess very small values of f but large or considerable values of k_0, which determine the ratings of LF. Pyrazolinylazo dyes with a large k_0 value, therefore, should be safely used in single dyeing or in mixture dyeing only with dyes with small values of f. Among the dyes examined, dyes with small values of both f and k_0 may be ideal reactive dyes.

3.8. Molecular descriptors for ene and [2 + 2] cycloaddition: photo-oxidative fading, its utility and limit

Applying the semiempirical MO theory to the pyrazolinylazo dyes and comparing their rates of fading on cellophane by Rose Bengal, how and to what extent the MO theory can describe the photo-oxidative reaction for the predominant tautomer were analysed.

According to frontier orbital theory, these reactions were analysed using a semiempirical MO PM5 method. The AHT of pyrazolinylazo dyes with *o*-hydroxy or *o*-amino groups was discussed by calculating the heat of formation for the A&HTs of these dyes in both the gas phase and water. The dyes with *o*-hydroxy groups were considered to exist as HTs in the gas phase and water as well as on cellulose.

The $S_{m,n}^{(E)}$ values given by Eq. (4) for the available double bonds ($C_m{=}C_n$), where duplicated sites are counted only once, describe the reactivity of a dye against singlet oxygen, a molecular descriptor for ene and/or [2 + 2] cycloaddition reactions for the reaction of azo dyes. Double bonds with larger values of $(f_m^{(E)} + f_n^{(E)})$ are taken into consideration one by one. The summation is performed from the position with the largest value of $(f_m^{(E)} + f_n^{(E)})$ to the position of the lowest limit. Since, although the relational factor may be smaller than unity, the electrophilic frontier density is proportional to $\log k_0$, the lowest limit may correspond to the measuring limit. When the values of $(f_m^{(E)} + f_n^{(E)})$ are large but either one of those of $f_r^{(E)}(r = m \text{ or } n)$ are smaller than a limit, the contribution of the atomic positions to the reaction is the subject to debate. The positions with small $f_r^{(E)}$ values should be excluded because of low reactivity, although whether or what factors it depended on or the limit could not be determined.

This procedure is not limited by a narrow range of chemical structures with one substituent each but may be applied to wider structures with more than one substituent than Hammett rule can. However, it was not be determined to what extent the range can be expanded.

From the viewpoint of molecular descriptors, the present procedure can be utilized for the molecular design of azo dyes with higher LF. Unlike the Hammett rule, the present procedure has no reference compounds. Although the introduction of frontier orbital energy may be one of the answers like superdelocalizability [26], no one may estimate the precise values as reactants on cellulose. The range of application may be wider than the Hammett rule, although the application beyond fundamental structures seems to show another linear correlation. According to Fukui's frontier orbital theory, the electrophilic reactivity of dyes is proportional to the sum of electron densities at the atomic positions of corresponding double bonds (Eq. (4)) in an unlimited range of chemical structures. This equation takes the effects of orbitals other than HOMO into consideration in the frontier electron densities, but those of differences in the HOMO energies, E_{HOMO}, which were related to superdelocalizability [26], among dyes examined were not considered. The dyes used in the present study possess a narrow range of E_{HOMO} (cf. Tables 2 and 3). In reality, the energy difference between the E_{HOMO} of dyes and the E_{LUMO} of singlet oxygen must be considered.

The molecular orbital calculation should be carried out for dyes on water-swollen cellulose. Since absorption spectra on the substrate are the same as those on dry cellulose but in water, the MO calculation was approximated by that in the gas phase due to the dielectric constant near the constant of gas phase.

Plots between $S_{m,n}^{(E)}$ values versus $\log k_0$ for the series of pyrazolinylazo dyes examined showed a good correlation between them. The absorption spectra of the

decomposed products bound with cellulose proved the predominant reaction mode except for the side reactions. The reactivity of azo dyes may be described by the frontier orbital theory, in which ene and [2 + 2] cycloaddition reactions are treated.

4. Summary

The fact that the reaction of pyrazolinylazo dyes with singlet oxygen formed decomposed products of definite structures may show that the reaction was ionic but not radical. From the absorption spectra of decomposed products by the photosensitised oxygenation reaction of the azo dyes bound with cellulose, the reaction schemes for the oxygenation reaction with singlet oxygen and for the photolysis and/or thermolysis of their intermediates were discussed.

According to frontier orbital theory, the reactivities of the predominant tautomers, the sites, mechanism and rates of reaction, were analysed for seven dyes. Their reactions with singlet oxygen occurred via ene and/or [2 + 2] cycloaddition. The rates of reaction estimated experimentally were demonstrated to have close relationships with the sum of electrophilic frontier densities of both atoms of the double bonds, which possess the reactivities. The absorption spectra of decomposed products proved the validity of these analyses.

Since pyrazolinylazo dyes possess fixed double bonds, the dyes with high reactivity toward singlet oxygen exhibit the highest reaction site at C1=C2 for ATs, C1=C5 for A/KTs and at C1=N6 and N4=C5 for HTs. Substituents that decrease the reactivity of the pyrazolinylazo dyes dispersed the d_{HOMO} at the sites into other atomic sites. Although one of the substituents was the *o*-sulfo group, its fulfillment required the introduction of other substituents at suitable positions. An introduction of such substituents has been found to develop pyrazolinylazo dyes with excellent LF, since pyrazolinylazo dyes possess low photosensitivity.

The molecular descriptor for the reactivity of azo dyes toward singlet oxygen was proved to be the $S^{(E)}_{m,n}$ values given by Eq. (2) based on Fukui's frontier orbital theory. The common relation line between $\log k_0$ and $S^{(E)}_{m,n}$values as the sum of electrophilic electron density at the double bonds with potential reactivity, demonstrated experimentally using seven dyes, may be an extension of the Hammett equation to the multi-substituent effect beyond single aromatic rings.

Acknowledgement

This work was supported by a Grant-in-Aid for Scientific Research by the Ministry of Education, Culture, Sports, Science and Technology, Japan.

References

[1] Hihara T, Okada Y, Morita Z. An analysis of azo-hydrazone tautomerism of reactive azobenzene and pyrazolinylazo dyes, using semiempirical molecular orbital PM5 method. Dyes and Pigments 2004;61(3):199–225.
[2] Hihara T, Okada Y, Morita Z. Azo-hydrazone tautomerism of phenylazonaphthol sulfonates and their analysis using semiempirical molecular orbital PM5 method. Dyes and Pigments 2003;59(1):25–41.
[3] Hihara T, Okada Y, Morita Z. Reactivity of phenylazonaphthol sulfonates, their estimation by semiempirical molecular orbital PM5 method, and the relation between their reactivity and azo-hydrazone tautomerism. Dyes and Pigments 2003;59(3):201–22.
[4] Garzillo C, Improta R, Peluso A. PM3 study of the electronic spectra of some substituted aminocoumarines. Journal of Molecular Structure: THEOCHEM 1998;426:145–53.
[5] Uchiyama S, Santa T, Okiyama N, Azuma K, Imai K. Semiempirical PM3 calculations predict the fluorescence quantum yields of 4-monosubstituted benzofurazan compounds. Journal of the Chemical Society, Perkin Transactions 2000;2:1199–207.
[6] Karelson M, Zerner MC. On the n–π* blue shift accompanying solvation. Journal of the American Chemical Society 1990;112:9405–6.
[7] Szafran M, Karelson MM, Katritzky AR, Koput J, Zerner MC. Reconsideration of solvent effects calculated by semiempirical quantum chemical methods. Journal of Computational Chemistry 1993;14(3):371–7.
[8] Morita Z, Hada S. A semiempirical molecular orbital study on the reaction of an aminopyrazolinyl azo dye with singlet molecular oxygen. Dyes and Pigments 1999;41(1):1–10.
[9] Okada Y, Hirose M, Kato T, Motomura H, Morita Z. Photofading of vinylsulfonyl reactive dyes on cellulose under wet conditions. Dyes and Pigments 1990;14:113–27.
[10] Hihara T, Okada Y, Morita Z. Relationship between photochemical properties and colourfastness due to light-related effects concerning monoazo reactive dyes derived from H-acid, γ-acid, and related naphthalene sulfonic acids. Dyes and Pigments 2004;60(1):23–48.
[11] Foote CF, Clennan EL. Properties and reaction of singlet dioxygen. In: Foote CF, Valentine JS, Greenberg A, Liebman JF, editors. Active oxygen in chemistry. Glasgow: Blackie Academic and Professional; 1995. p. 105–40 [chapter 4].
[12] Gorman AA, Rogers MAJ. Singlet oxygen. In: Scaiano JC, editor. CRC handbook of organic photochemistry, vol. II. Boca Raton: CRC Press; 1989. p. 229–47.
[13] Rosenthal I. Chemical and physical sources of singlet oxygen. In: Frimer AA, editor. Singlet O_2, Physical–chemical aspects, vol. 1. Boca Raton: CRC Press; 1985. p. 13–38 [chapter 2].
[14] Bonnett R. Photosensitizers of the porphyrin and phthalocyanines series for photodynamic therapy. Chemical Society Review 1995;19–33.
[15] DeRosa MC, Crutchley RJ. Photosensitized singlet oxygen and its applications. Coordination Chemistry Reviews 2002;233–234:351–71.
[16] Okada Y, Hirose M, Kato T, Motomura H, Morita Z. Fading of vinylsulfonyl reactive dyes on cellulose in admixture under wet conditions. Dyes and Pigments 1990;14:265–85.
[17] Ganster J, Fink H-P. Physical constants of cellulose. In: Brundrup J, Immergut EH, Grulke EA, editors. Polymer handbook. 4th ed. New York: Wiley; 1999. p. V/135–57.
[18] Mehta RH. Physical constants of various polyamides. In: Brundrup J, Immergut EH, Grulke EA, editors. Polymer handbook. 4th ed. New York: Wiley; 1999. p. V/121–33.
[19] Frimer AA. The reaction of singlet oxygen with olefins: the question of mechanism. Chemical Reviews 1979;79:359–87.

[20] Frimer AA, Stephenson LM. The singlet oxygen ene reaction. In: Frimer AA, editor. Singlet O_2, Reaction modes and products, Part 1, vol. II. Boca Raton: CRC Press; 1985. p. 68–91 [chapter 3].
[21] Yamaguchi K. Theoretical calculations of singlet oxygen reactions. In: Frimer AA, editor. Singlet O_2, vol. III. Reaction modes and products, Part 2. Boca Raton: CRC Press; 1985. p. 119–251 [chapter 2].
[22] Gollnick K, Kuhn HJ. Ene-reactions with singlet oxygen. In: Wassermann HH, Murray RW, editors. Singlet oxygen. New York: Academic Press; 1979. p. 287–427.
[23] Orfanopoulos M. Singlet oxygen ene-sensitizer photo-oxygenations: Stereochemistry and mechanism. Molecular and supramolecular photochemistry 2001;8:243–85.
[24] Bloodworth J, Eggelte HJ. Endoperoxide. In: Frimer AA, editor. Singlet O_2, vol. II. Reaction modes and products, Part 1. Boca Raton: CRC Press; 1985. p. 93–203 [chapter 4].
[25] Griesbeck AG, El-Idreesy TT, Adam W, Krebs O. Ene-reactions with singlet oxygen. In: Horspool WM, Lenci F, editors. CRC handbook of organic photochemistry and photobiology. 2nd ed. Boca Raton: CRC Press; 2003. p. 8-1–8-20 [chapter 8].
[26] Fukui K, Fujimoto H. Frontier orbitals and reaction paths. Singapore: World Scientific; 1997.
[27] Fukui K, Yonezawa T, Shingu H. A molecular orbital theory of reactivity in aromatic hydrocarbons. Journal of Chemical Physics 1952;20(4):722–5.
[28] Fukui K, Yonezawa T, Nagata C, Shingu H. Molecular orbital theory of orientation in aromatic, heteroaromatic and other conjugated molecules. Journal of Chemical Physics 1954; 22(8):1433–42.
[29] Fukui K, Yonezawa T, Nagata C. Interrelations of quantum-mechanical quantities concerning chemical reactivity of conjugated molecules. Journal of Chemical Physics 1957; 26(4):831–41.
[30] CAChe Reference Guide 2002, 4.9; 3-9–3-10, Fujitsu Ltd.
[31] Griffiths J, Hawkins C. Oxidation by singlet oxygen of arylazonaphthols exhibiting azo-hydrazone tautomerism. Journal of the Chemical Society, Perkin Transactions 2, 1977;(6):747–52.
[32] Rembold MW, Kramer HEA. Singlet oxygen as an intermediate in the catalytic fading of dye mixtures. Journal of the Society of Dyers and Colourists 1978;94(1):12–7.
[33] Griffiths J, Hawkins C. Synthesis and photochemical stability of 1-phenylazo-2-naphthol dyes containing insulated singlet oxygen-quenching groups. Journal of Applied Chemistry and Biotechnology 1977;27:558–64.
[34] Lyčka A, Macháček V. ^{13}C and ^{15}N-NMR studies of the azo–hydrazone tautomerism of some azo dyes. Dyes and Pigments 1986;7(3):171–85.
[35] Mustroph H, Weiss C. Fading behavior of tautomerizable azo dyes. IV. Quantum-chemical calculations for the photofading mechanism of 1-phenylazo-naphthols. Zeitschrift für Chemie 1983;23(2):61–2.
[36] Mustroph H, Potocnak J, Grossmann N. Studies of the photochemical fading of tautomeric azo dyes. VI. Photochemical oxidation of phenylazoacetylacetones and phenylazopyrazolones by singlet oxygen. Journal für praktische Chemie 1984; 326(6):979–84.
[37] Mustroph H, Weisss C. Investigations of the photofading of tautomeric azo dyes. VIII. Quantum chemical calculations for the fading behavior of hydrazones. Journal für praktische Chemie 1986;328(5–6):937–40.
[38] Okada Y, Kato T, Motomura H, Morita Z. Fading mechanism of reactive dyes on cellulose by simultaneous effects of light and perspiration. Sen'i Gakkaishi 1990;46(8):346–55.
[39] Okada Y, Morita Z. Fading of some vinylsulfonyl reactive dyes on cellulose under various conditions. Dyes and Pigments 1992;18(4):259–70.
[40] Okada Y, Sato E, Motomura H, Morita Z. Photofading of monochlorotriazinyl reactive dyes on cellulose under wet conditions. Dyes and Pigments 1992;19(1):1–19.
[41] Okada Y, Orikasa K, Motomura H, Morita Z. Oxidative and reductive fading of monochlorotriazinyl reactive dyes on cellulose under wet conditions. Dyes and Pigments 1992; 19(3):203–14.
[42] Okada Y, Fukuoka F, Morita Z. Environmental effects of oxygen on the fading of monochlorotriazinyl reactive dyes on cotton fabrics. Dyes and Pigments 1998;37(1):47–64.
[43] Stephenson LM. The mechanism of the singlet oxygen ene reaction. Tetrahedron Letters 1980;21(11):1005–8.
[44] Stratakis M, Orfanopoulos M, Foote CS. Solvent effects in the stereoselectivity of the ene reaction of singlet oxygen with allylic alcohols. Tetrahedron Letters 1996;37(40):7159–62.
[45] Vassilikogiannakis G, Stratakis M, Orfanopoulos M, Foote CS. Stereochemistry in the ene reactions of singlet oxygen and triazolindiones with allelic alcohols: a mechanistic comparison. Journal of Organic Chemistry 1999;64(11):4130–9.
[46] Dewar MJS, Thiel W. Ground states of molecules. XXX. MINDO/3 study of reactions of singlet ($^1\Delta_g$) oxygen with carbon–carbon double bonds. Journal of the American Chemical Society 1975;97(14):3978–86.
[47] Grdina MB, Orfanopoulos M, Stephenson LM. Stereochemical dependence of isotope effects in the singlet oxygen–olefin reactions. Journal of the American Chemical Society 1979;101(11):3111–2.
[48] Jursic BS, Zdravkovski Z. Reaction of imidazoles with ethylene and singlet oxygen. An ab initio theoretical study. Journal of Organic Chemistry 1995;60(9):2865–9.
[49] Sevin F, McKee ML. Reactions of 1,3-cyclohexadiene with singlet oxygen. A theoretical study. Journal of the American Chemical Society 2001;123(19):4591–600.
[50] Bobrowski M, Liwo A, Ołdzjiej S, Jeziorek D, Ossowski T. CAS MCSCF/CAS MCQDPT2 study of the mechanism of singlet oxygen addition to 1,3-butadiene and benzene. Journal of the American Chemical Society 2000;122(34):8112–9.
[51] Clennan EL, Nagraba K. The addition of singlet oxygen to alkoxy substituted dienes. The mechanism of singlet oxygen 1,2-cycloaddition reaction. Journal of the American Chemical Society 1988;110:4312–8.
[52] Lay TH, Bozzelli JW. Enthalpies of formation of cyclic alkylperoxides: dioxetane, 1,2-dioxetane. Chemical Physics Letters 1997;268(12):175–9.
[53] Liwo A, Dyl D, Jeziorek D, Nowacka M, Ossowski T, Woźnicki W. MCSCF study of singlet oxygen addition to ethanol – a model of photooxidation reactions of unsaturated and aromatic compounds bearing hydroxy groups. Journal of Computational Chemistry 1997;18(13):1668–81.
[54] Baumstark AL. The dioxetane ring system: preparation, thermolysis, and insertion reactions. In: Frimer AA, editor. Singlet O_2, vol. II. Boca Raton: CRC Press; 1985. p. 1–35.
[55] Adam W, Beinhauer A, Hauer H. Activation parameters and excitation yields of 1,2-dioxetane chemiluminescence. In: Scaiano JC, editor. Handbook of organic photochemistry, vol. 2. Boca Raton: CRC Press; 1989. p. 271–327 [chapter 12].
[56] Takano Y, Tsunesada T, Isobe H, Yoshioka Y, Yamaguchi K, Saito I. Theoretical studies of decomposition reactions of dioxetane, dioxetanone, and related species. CT induced luminescence mechanism revisited. Bulletin of the Chemical Society of Japan 1999;72:213–25.
[57] Tanaka C, Tanaka J. Ab initio molecular orbital studies on the chemiluminescence of 1,2-dioxetanes. Journal of Physical Chemistry A 2000;104(10):2078–90.
[58] Vasil'ev RF. Changes of structure and energy on the route from dioxetane to carbonyl products. A quantum chemical study.

Journal of Bioluminescence and Chemiluminescence 1998;13(2):69–74.
[59] Wilsey S, Bernardi F, Olivucci M, Robb MA, Murphy S, Adam W. Thermal decomposition of 1,2-dioxetane revisited. Journal of Physical Chemistry A 1999;103(11):1669–77.
[60] Baumstark AL, Andersen SL, Sapp CJ, Vaquez PC. Thermolysis of 3-alkyl-3-methyl-1,2-dioxetanes: activation parameters and chemiexcitation yields. Heteroatom Chemistry 2001; 12(6):459–62.
[61] Adam W, Bosio SG, Turro NJ. Highly diastereoselective dioxetane formation in the photooxygenation of enecarbamates with an oxazolindinone chiral auxiliary. Journal of the American Chemical Society 2002;124(30):8814–5.
[62] Rodoriguez E, Reguero M. The DDCI method applied to reactivity: chemiluminescent decomposition of dioxetanes. Journal of Physical Chemistry A 2002;106(3):504–9.
[63] Cermola F, Iesce MR. Substituent and solvent effects on the photosensitised oxygenation of 5,6-dihydro-1,4-oxahiins. Intramolecular oxygen transfer vs. normal cleavage of the dioxetane intermediates. Journal of Organic Chemistry 2002;67(4):4937–44.
[64] Reguero M, Bernardi F, Bottoni A, Olivucci M, Robb MA. Chemiluminescent decomposition of 1,2-dioxetanes: An MC-SCF/MP2 study with VB analysis. Journal of the American Chemical Society 1991;113(5):1566–72.
[65] Adam W, Saha-Möller CR, Schönberger A. Type I and type II photosensitised oxidative modifications of 2′-deoxyguanosine by triplet-excited ketones generated thermally from the 1,2-dioxatane HTMD. Journal of the American Chemical Society 1997;119(4):719–23.
[66] Orfanopoulos M, Smonou I, Foote CS. Intermediates in the ene reactions of singlet oxygen and *N*-phenyl-1,2,4-triazoline-3,5-dione with olefins. Journal of the American Chemical Society 1990;112(9):3607–14.
[67] Duchstein H-J, Ruch-Zaske G, Holzmann G, Wollenberg E, Weber H. Die Reaktion von Sigulett-Sauerstoff mit 4-Amino-3-pyrazolin-5-onen. Archiv der Pharmazie (Weinheim) 1988;321:25–7.
[68] Akasaka T, Nakagawa M, Nomura Y, Sato R, Someno K, Ando W. Reaction of singlet oxygen with 2-pyrazolin: implication for cation radical-superoxide ion pair intermediate. Tetrahedron 1986;42(14):3807–12.
[69] Karelson M. Molecular descriptors in QSAR/QSPR. New York: Wiley-Interscience; 2000.
[70] Engel PS. Mechanism of the thermal and photochemical decomposition of azoalkanes. Chemical Reviews 1980;80(4): 99–150.
[71] Zollinger H. Diazo chemistry I, aromatic and heteroaromatic compounds. Weinheim: VCH; 1994.
[72] Forstinger K, Metz HJ. Diazo compounds and diazo reactions. 6th ed. In: Ullmann's encyclopedia of industrial chemistry, vol. 10 Weinheim: Wiley–VCH; 2002. p. 497–517.
[73] Lutz W, Bräuninger A. Imaging technology. 6th ed. In: Ullmann's encyclopedia of industrial chemistry, vol. 17 Weinheim: Wiley–VCH; 2002. p. 387–492 (authors of related section: Technical copying).
[74] Zollinger H. Color chemistry. 3rd revised ed. Weinheim: Wiley–VCH; 2003.
[75] Bravo-Díaz C, Romero EG. Reactivity of arenediazonium ions in micellar and macromolecular systems. Current Topics in Colloid and Interface Science 2001;4:57–83.
[76] Müller U, Utterrodt A, Mörke W, Deubzer B, Herzig Ch. Diazonium salts as cationic photoinitiators: radical and cationic aspects, In: Belfield KD, Crivello JV, editors. ACS Symposium Series 2003; 847 (photoinitiated polymerization). p. 202–12 [chapter 17].
[77] Klessinger M, Michl J. Excited states and photochemistry of organic molecules. New York: VCH; 1995 [7.2.2: N2 elimination from azo compounds].
[78] Smith MB, March J. March's advanced organic chemistry. 5th ed. New York: VCH; 2001 [11–32: Migration of the nitroso group: The Fischer–Hepp rearrangement].
[79] Hihara T, Okada Y, Morita Z. Photo-oxidation and -reduction of vat dyes on water-swollen cellulose and their lightfastness on dry cellulose. Dyes and Pigments 2002;53(2):153–77.